2010-12-14

Hydraulic Conductivity of Cement-Treated Soils and Aggregates after Freezing

Michael Scott Shea
Brigham Young University - Provo

Hydraulic Conductivity of Cement-Treated Soils and Aggregates after Freezing

M. Scott Shea

A thesis submitted to the faculty of
Brigham Young University
in partial fulfillment of the requirements for the degree of

Master of Science

W. Spencer Guthrie, Chair
Mitsuru Saito
Gustavious P. Williams

Department of Civil and Environmental Engineering

Brigham Young University

April 2011

ABSTRACT

Hydraulic Conductivity of Cement-treated Soils

and Aggregates after Freezing

M. Scott Shea

Department of Civil and Environmental Engineering

Master of Science

Improvements in the strength and durability of frost-susceptible soils and aggregates can be achieved through chemical stabilization using portland cement, where the efficacy of cement stabilization for improving durability depends on the degree to which hydraulic conductivity is reduced. Hydraulic conductivity is commonly estimated from basic soil properties using Moulton's empirical equation. However, the hydraulic conductivity estimation does not consider the detrimental effects of freezing or the benefits of cement stabilization. The purpose of this research was to derive new equations relating hydraulic conductivity after freezing to specific material properties of cement-treated soils and aggregates stabilized with different concentrations of cement.

This research included material samples from two locations in Alaska and from single locations in Minnesota, Montana, Texas, and Utah, for a total of six material samples. Each soil or aggregate type was subjected to material characterization by the Unified Soil Classification System (USCS) and the American Association of State Highway and Transportation Officials (AASHTO) classification system. Moisture-density curves were developed, and unconfined compressive strength (UCS) testing was performed to determine cement concentrations generally corresponding to low, medium, and high 7-day UCS values of 200, 400, and 600 psi, respectively. After being cured for 28 days at 100 percent relative humidity, the prepared specimens were subjected to frost conditioning and hydraulic conductivity testing.

The Alaska-Elliott, Minnesota, Montana, and Utah materials exhibit decreasing hydraulic conductivity with increasing UCS, the Texas material exhibits increasing hydraulic conductivity with increasing strength from the low to medium cement concentration levels but decreasing hydraulic conductivity from the medium to high cement concentration levels, and the Alaska-Dalton material exhibits increasing hydraulic conductivity with increasing strength.

Multivariable regression analyses were performed to investigate relationships between hydraulic conductivity and several material properties, including soil gradation and

classification, fineness modulus, specific gravity, cement content, porosity, compaction method, dry density, and 7-day UCS for each specimen. The R^2 values computed for the six-parameter, four-parameter, USCS, and AASHTO-classification models are 0.795, 0.767, 0.930, and 0.782, respectively. Further research is recommended to investigate the effects of cement on hydraulic conductivity for USCS and AASHTO soil types not covered in this research.

Key words: cement treatment, frost action, hydraulic conductivity, permeability

ACKNOWLEDGMENTS

Appreciation and thanks go to Dr. W. Spencer Guthrie for his exceptional guidance and expertise. I offer my gratitude to David Anderson for his assistance in performing experiments. Dr. Dennis Eggett was instrumental in the statistical analysis and consultation. Many peers helped me at different stages in this research. My daughters Betsy and Avie gave me moral support and cheerleading throughout my graduate work. Greatest acknowledgement and thanks go to my wife, Mickelle, who inspired me through my graduate work with love, patience, and encouragement.

TABLE OF CONTENTS

LIST OF TABLES

LIST OF FIGURES

1 INTRODUCTION

1.1 Problem Statement

Water movement through soils and aggregates comprising pavement structures can cause material degradation, resulting in reduced bearing capacity and accelerated development of distress. In cold climates, in particular, moisture infiltration results in frost damage manifested as frost heave and surface roughness during winter and thaw-weakening during spring (*1*). Damage from frost heave increases when the thawing of frozen soils and aggregates creates supersaturated conditions in the upper layers of the pavement structure; moisture does not readily permeate through the still-frozen underlying layers, and the supersaturated conditions reduce the bearing capacity of the pavement system (*2, 3, 4, 5*). Frost heave and the secondary effects of heave deteriorate the pavement structure at an accelerated rate.

The use of chemical stabilizers can mitigate the effects of frost action in pavements. Stabilization is often accomplished through the use of cement treatment, which involves mixing a specified quantity of portland cement into the soil or aggregate material and compacting the blend to a specified density. The soil-cement or cement-treated base (CTB) product then becomes a durable pavement layer with increased structural capacity (*6*). Research in cement treatment has verified that properly designed CTB materials exhibit negligible frost heave and experience minimal spring-thaw weakening (*7, 8, 9*).

Damage mechanisms associated with water movement are largely dependent on the hydraulic conductivity, or permeability to water, of the affected layers. The efficacy of cement stabilization for improving durability therefore depends on the degree to which hydraulic conductivity is reduced (*10*). Designers typically determine cement concentrations based strictly on strength measurements, without regard to hydraulic conductivity (*11*). Hydraulic conductivity can be measured in a laboratory by monitoring the amount of water that flows through a soil or aggregate specimen of known length and cross-sectional area, due to an imposed hydraulic head. However, hydraulic conductivity measurements require specialized laboratory equipment, and the testing is relatively time-consuming and therefore expensive. Consequently, basic material properties such as grain-size distribution, specific gravity (SG), and dry density are sometimes used to estimate hydraulic conductivity with Moulton's or Cedergren's empirical equations, for example (*12*). However, the hydraulic conductivity estimation does not consider the detrimental effects of freezing or the benefits of cement stabilization. Research indicates that hydraulic conductivity can increase by an order of magnitude or more as a result of the first freeze-thaw cycle; crack networks form and physically change the soil fabric (*10*).

The purpose of this research was to derive new equations relating hydraulic conductivity after freezing to specific material properties of cement-treated soils and aggregates stabilized with different concentrations of cement. This work will particularly benefit pavement and materials engineers working in regions in which frost action is prevalent.

1.2 Scope

This research included material samples from two locations in Alaska and from single locations in Minnesota, Montana, Texas, and Utah, for a total of six material samples (*7, 13*). The sample materials were strategically chosen to represent a range of moisture- and frost-susceptibility characteristics. Each material was mixed with different amounts of cement to achieve low, medium, and high 7-day compressive strengths approximately equal to 200, 400, and 600 psi, respectively. The prepared specimens were subjected to frost conditioning and hydraulic conductivity tests following experimental methods developed in this research. A stepwise regression was performed on the data to produce equations relating post-freezing hydraulic conductivity to specific material properties.

1.3 Outline

This report contains five chapters. Chapter 1 describes the research objective and scope, and Chapter 2 gives background information on hydraulic conductivity and the effects of cement treatment. Chapter 3 outlines material characterization, preparation, and testing procedures employed in the research, and Chapter 4 provides the results of material testing and statistical analyses. Chapter 5 gives conclusions and recommendations.

2 BACKGROUND

2.1 Overview

This chapter discusses frost susceptibility and the mitigation of frost damage through the use of cement treatment. A discussion of the effects of cement treatment on hydraulic conductivity is also given.

2.2 Frost Susceptibility

The frost susceptibility of a soil or aggregate can be classified using the U.S. Army Corps of Engineers criteria presented in Table 2-1 (*1*). The susceptibility to frost damage is determined from the percentage by mass of material finer than 0.02 mm and from the soil classification determined using the Unified Soil Classification System (USCS). Soils are listed in Table 2-1 in approximate order of increasing frost susceptibility under freezing conditions or decreasing bearing capacity during thawing.

Frost-susceptible soils and aggregates can experience damage through two mechanisms, sustained freezing and freeze-thaw cycling (*1, 6, 12, 14*). The freezing of subsurface soil water nucleates ice crystals in the vadose zone at or near the ground surface (*15, 16, 17, 18*). In conditions of sustained freezing, the development of cryosuction in the freezing zone then causes soil water from deeper unfrozen soil strata to be drawn towards the freezing front (*19, 20*). As

Table 2-1: Frost Susceptibility Classifications of Soil

Frost Group	Kind of Soil	Percentage Finer than 0.02 mm by Weight	Typical Soil Types under USCS
NFS	(a) gravel crushed stone crushed rock	0-1.5	GW, GP
	(b) sand	0-3	SW, SP
PFS	(a) gravel crushed stone crushed rock	1.5-3	GW, GP
	(b) sand	3-10	SW, SP
S1	gravelly soil	3-6	GW, GP, GW-GM, GP-GM
S2	sandy soil	3-6	SW, SP, SW-SM, SP-SM
F1	gravelly soil	6-10	GM, GW-GM, GP-GM
F2	(a) gravelly soil	10-20	GM, GW-GM, GP-GM
	(b) sand	6-15	SM, SW-SM, SP-SM
F3	(a) gravelly soil	over 20	GM, GC
	(b) sand, except very fine silty sand	over 15	SM, SC
	(c) clay, PI>12	-	CL, CH
F4	(a) all silts	-	ML, MH
	(b) very fine silty sands	over 15	SM
	(c) clay, PI>12	-	CL, CL-ML
	(d) varved clay and fine-grained banded sediment	-	CL or CH banded with ML, MH or SM layers

the incoming water freezes, a volumetric expansion of 9 percent occurs as the liquid water changes to ice. Continual ingress and freezing of water lead to the formation of ice lenses that cause segregation and differential displacement, or frost heave, of the soil (*21, 22*). During spring thaw, the excess moisture in upper soil layers cannot drain through the still-frozen lower layers, causing a marked reduction in the strength of the thawed soil and accelerated damage under trafficking (*3, 6, 19*).

In conditions of freeze-thaw cycling, material degradation occurs as in-situ water repeatedly expands with each freeze (*10, 15*). When the volume of ice and supercooled water in

a given pore exceed the available pore space, the soil matrix is disrupted as soil particles are forced apart (*20*). This process results in increased susceptibility of the soil to water ingress and additional damage from freeze-thaw cycling (*23*).

2.3 Cement Treatment

Treatment with portland cement is one common method of improving the strength and durability of frost-susceptible soils and aggregates. Portland cement is mixed with the material at a specified weight ratio to achieve desired improvements (*8*). Previous research has shown that sufficient additions of portland cement can significantly increase the resistance of materials to damage under both sustained freezing and freeze-thaw cycling (*7, 24, 25, 26*).

In addition to binding soil and aggregate particles together, the addition of a proper concentration of cement also yields a reduction in the hydraulic conductivity of the treated material (*27*). The optimum amount of cement for a given soil or aggregate depends on the soil properties and service conditions in which it will be placed but generally corresponds to 7-day unconfined compressive strengths (UCS) ranging from 200 to 600 psi. While insufficient cement leads to poor durability, excessive cement can cause shrinkage cracking of the cement-treated layer and therefore lead to increased water flow through the layer (*7, 8, 25*).

2.4 Hydraulic Conductivity

Hydraulic conductivity is a measure of the rate at which water can flow through a soil or aggregate. Materials characterized by low porosity and high tortuosity have lower hydraulic conductivities than materials with more interconnected voids (*26*). The amount of voids and the geometry of pore water pathways in a soil or aggregate matrix are influenced by particle-size

distributions, the degree of compaction, and the presence of hydration products in cement-treated materials (*10, 28*). Therefore, in such cases, hydraulic conductivity is theoretically a function of soil classification, dry density, and cement concentration, which are in many ways inter-dependent (*12*). The soil classification reflects the maximum dry density that can be attained under a given compaction effort and is used in specifications of cement concentrations. The maximum dry density is also affected by the presence of cement, which can change the particle-size distribution and related characteristics of a soil or aggregate (*27, 28*). In addition, frost action can cause changes in the dry density of such materials (*8, 10*). Investigating the hydraulic conductivity of frost-conditioned, cement-treated soils and aggregates, based on these issues, was the objective of this research.

2.5 Summary

The frost susceptibility of a soil or aggregate can be classified using the U.S. Army Corps of Engineers criteria. Frost-susceptible soils and aggregates experience damage through sustained freezing and freeze-thaw cycling. In both cases, as subsurface water freezes, a volumetric expansion of 9 percent occurs as the liquid water changes to ice. The formation of ice can cause frost heave of affected pavement structures and degradation of the pavement materials. These processes can result in increased susceptibility of the materials to water ingress and additional frost damage. Treatment with portland cement is one common method of improving the strength and durability of frost-susceptible soils and aggregates. The addition of a proper amount of cement yields a reduction in the hydraulic conductivity of the treated material.

3 PROCEDURES

3.1 Overview

This chapter outlines the procedures used in this research for material characterization, moisture-density relationships, cement concentrations, and hydraulic conductivity testing. In addition, the statistical analyses utilized in this research are described.

3.2 Material Characterization

Each of the six materials evaluated in this research was received in bulk from the respective sources, oven-dried at 140°F, and then separated using 0.75-in., 0.50-in., 0.375-in., No. 4, 8, 16, 30, 50, 100, and 200 sieves in order to obtain a bulk gradation for each material. All samples of a given material were subsequently prepared using the same bulk gradation to ensure consistency.

Material classifications were conducted according to the USCS in general accordance with American Society for Testing and Materials (ASTM) D2487 (Standard Classification of Soils for Engineering Purposes) and the American Association of State Highway and Transportation Officials (AASHTO) system using AASHTO M145 (Standard Classification of Soils and Soil-Aggregate Mixtures for Highway Construction Purposes). Both classifications require knowledge of particle-size distributions and Atterberg limits. Particle-size distributions were measured in general accordance with ASTM D2217 (Standard Practice for Wet Preparation

of Soil Samples for Particle-Size Analysis and Determination of Soil Constants) and ASTM D422 (Standard Test Method for Particle-Size Analysis of Soils). Atterberg limits and SG were determined in general accordance with ASTM D4318 (Standard Test Method for Liquid Limit, Plastic Limit, and Plasticity Index of Soils) and ASTM D854 (Standard Test Methods for Specific Gravity of Soil Solids by Water Pycnometer), respectively.

3.3 Moisture-Density Relationships

Moisture-density curves were developed by mixing and compacting 4-in.-diameter specimens with 4.6-in. heights at various moisture contents. Each sample was prepared following the bulk gradation previously established for the given material, moistened to a water content of interest, and allowed to equilibrate for 24 hours before being compacted. The standard Proctor procedure described in ASTM D698 (Standard Test Methods for Laboratory Compaction Characteristics of Soil Using Standard Effort) was utilized in this research for soils, while the modified Proctor procedure described in ASTM D1557 (Standard Test Methods for Laboratory Compaction Characteristics of Soil Using Modified Effort) was utilized for aggregates; the standard Proctor method was used for the materials from Montana and Utah, and the modified Proctor method was used for the materials from Alaska, Minnesota, and Texas. After compaction, five additional blows were applied to each specimen with a finishing tool to level and smooth the surface. Figure 3-1 displays the compaction hammer and finishing tool used in this research.

Figure 3-1: Compaction hammer and finishing tool.

The height and weight of each compacted specimen were then measured to facilitate calculation of wet density. Following extrusion from the mold, each specimen was oven-dried at 230°F to determine gravimetric water content, which was used with the wet density measurement to compute dry density. The dry density and moisture content of each specimen were plotted to determine the optimum moisture content (OMC) and maximum dry density (MDD) for each material. At least three specimens per material were tested at varying moisture contents.

3.4 Cement Concentrations

After the OMC and MDD were determined for each untreated material, preliminary cement concentrations were chosen to obtain a general relationship between cement content and 7-day UCS in the range of 200 to 600 psi for each material. Samples were again prepared following the appropriate bulk gradation, but particles coarser than the No. 4 sieve were weighed out separately from those finer than the No. 4 sieve. The fraction of the material coarser than the

No. 4 sieve was soaked for 24 hours in an amount of water corresponding to the OMC for the sample, while the fraction finer than the No. 4 sieve was retained in a dry state. The OMC for the sample was estimated by multiplying the selected cement content, in percent, by 0.3 and adding that many percentage points to the OMC determined for the untreated material. At the conclusion of the soaking period, the specified amount of Type I/II portland cement was mixed with the fine fraction, which was then blended with the previously moistened coarse fraction. The samples were manually mixed until they appeared uniform in color and texture. They were then immediately compacted using the same protocols followed in determination of moisture-density relationships, including measurement of both height and weight. At least four specimens of each material were evaluated at varying cement contents.

Following compaction, the specimens were cured for 7 days in a fog room at 100 percent relative humidity and then, with the exception of the Montana material, soaked under water for 4 hours before being capped with high-strength gypsum; specimens prepared with the Montana material could not withstand the soaking, so those specimens were not submerged before UCS testing. The UCS of each specimen was then measured following ASTM D1633 (Standard Test Methods for Compressive Strength of Molded Soil-Cement Cylinders) at a strain rate of 0.05 in./minute.

Based on the measured relationships between cement concentrations and UCS, values for cement concentration generally corresponding to target 7-day UCS values of 200, 400, and 600 psi were chosen for each material. Selections were made so that the difference between low and medium levels of cement was equal to the difference between medium and high levels of cement in each case. These three levels of cement treatment represent low, medium, and high concentrations typical of values utilized in construction projects nationwide and are consistent

with previous research performed at Brigham Young University (BYU) (*7*, *13*). In selected instances, data were available from previously tested samples for which limited material remained at the time of the current study. In those cases, although the three cement concentration levels did not necessarily correspond to the target 7-day UCS values selected for evaluation in the current research, the data were still included. Three additional specimens were then prepared and tested for 7-day UCS at each of the selected cement contents, with the exception of the Texas material for which an insufficient quantity was available.

3.5 Hydraulic Conductivity Testing

After cement contents corresponding to the target 7-day UCS values were selected for each material type, larger specimens were prepared for hydraulic conductivity testing; these specimens were compacted at OMC in 6-in.-diameter plastic molds to a height of 9 in. Three replicate specimens were compacted at each of the three cement contents selected for evaluation of each material, for a total of nine specimens per soil type. As depicted in Figure 3-2, the plastic molds were pre-drilled with seven 0.125-in.-diameter holes in a circular pattern in the bottom to allow water uptake during the frost conditioning applied to each specimen. Filter paper was placed in the bottom of each mold to prevent fines from washing out of the holes during testing. Each empty mold was weighed with the filter paper prior to compaction to facilitate later calculation of specimen densities.

The number of lifts specified for compaction of a normal specimen, as defined in ASTM D698 or D1557, was doubled to achieve the target specimen height of 9 in. specified for this research. As before, five additional blows were applied with a finishing tool to level and smooth

Figure 3-2: Pre-drilled plastic molds.

the surface of each compacted specimen, and the height and weight were then measured. The specimens were then cured for 28 days at 100 percent relative humidity.

After the specified curing period was completed, each prepared specimen was subjected to frost conditioning comprised of a sustained freeze, in which a thermal gradient was imposed over the length of the specimen, and a rapid freeze, in which the entire specimen was completely frozen. The frost exposure was consistent with typical frost heave testing performed at the BYU Highway Materials Laboratory, in which specimens are insulated laterally, placed in a shallow water bath, and then subjected to a constant freezing surface temperature of 19°F for 10 days; Figure 3-3 shows the frost heave chamber utilized for this aspect of the frost conditioning (*7*). After completion of this phase, the specimens were removed from the environmental chamber,

Figure 3-3: Frost heave chamber.

unwrapped but retained inside their molds, placed directly into a chest freezer maintained at a temperature of 1.4°F for a duration of at least 24 hours, and then removed for thawing.

After frost conditioning, the specimens were removed from their molds using a rotary cutter as shown in Figure 3-4. Several layers of plastic wrap were then applied around the circumference of each specimen as shown in Figure 3-5. The plastic wrap served as a means of minimizing preferential flow between the exterior of the specimen and the inside walls of the polyvinyl chloride (PVC) pipe in which the specimens were enclosed within the permeameter utilized in this research. The 6-in.-diameter PVC pipe, approximately 10 in. in length, was cut longitudinally into two sections and held tightly around each specimen with two hose clamps. Excess plastic wrap extending beyond the ends of a specimen was wrapped back onto the PVC pipe so that the ends of the specimen were fully exposed as shown in Figure 3-6. This procedure minimized disturbance to the specimens.

Figure 3-4: Rotary cutter.

Figure 3-5: Specimen wrapped in plastic.

Figure 3-6: Specimen installed in PVC pipe.

The lower assembly of the permeameter, shown in Figure 3-7, was prepared so that the lower surface of a specimen would be equal in elevation to the flow path in the raised pipe section downstream of the valve; the matching water tables are indicated on both sides of the figure. De-ionized, de-aired water was then poured into the pipe system to fill the lower part of the permeameter. The ball valve, located at the lowest point in the system, was then closed to prevent drainage of the water during the specimen soaking process.

A specimen to be tested was then installed in the PVC pipe, which was in turn connected to the prepared lower assembly of the permeameter using a flexible coupler and hose clamp. A metal screen and filter paper were situated immediately beneath the specimen to prevent fines from being washed out of the specimen during testing (*29, 30*). Another flexible coupler was

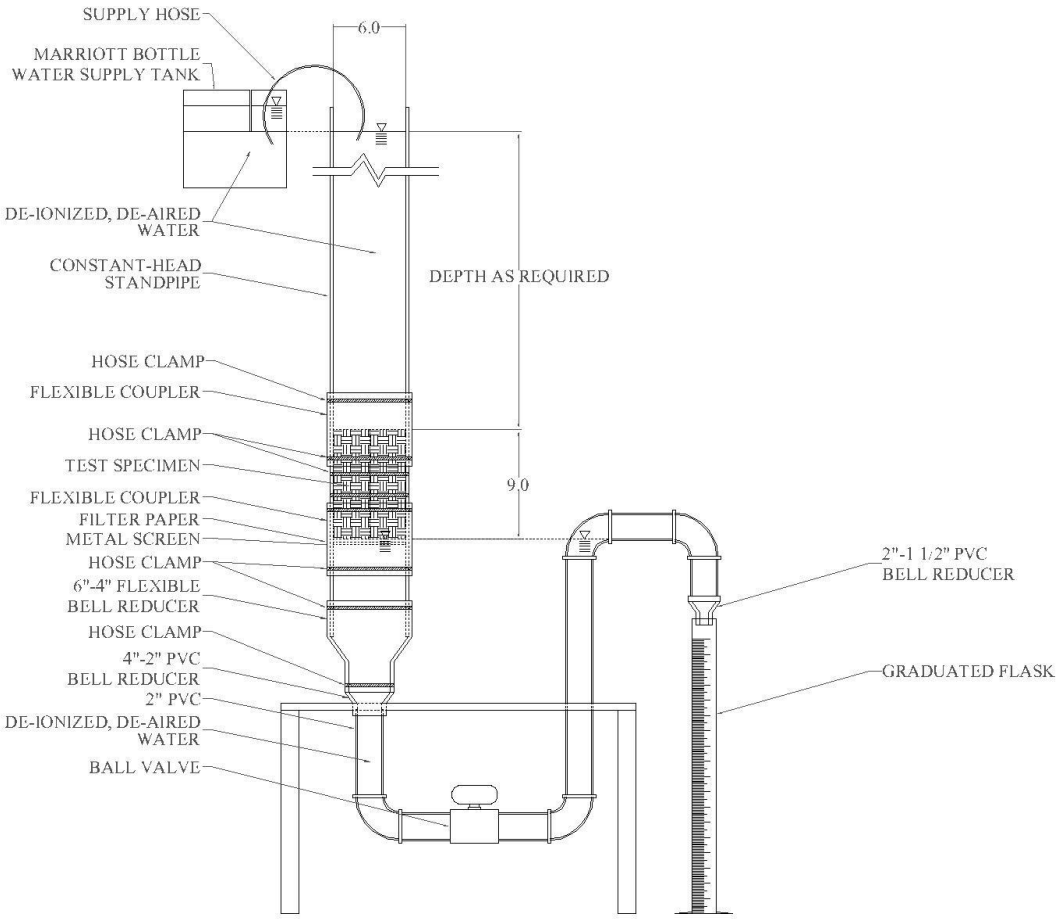

Figure 3-7: Schematic of permeameter.

used to connect an open 20-in. or 60-in. standpipe to the top of the specimen, and the standpipe was then filled with de-ionized, de-aired water to a height of 18 in. above the upper surface of the specimen. The specimen was allowed to soak in this condition for 4 hours. The upper assembly was then drained and dismantled, and the specimen was removed, still in the PVC pipe, so that the base of the specimen could be inspected. If the specimen appeared to be completely wetted, it was returned to the permeameter for hydraulic conductivity testing. If the specimen was not completely wetted after 4 hours, it was returned to the permeameter for an additional

20-hour soaking period, giving a total of 24 hours of soaking, and the inspection process was repeated. No specimen required more than 24 hours of soaking to achieve satisfactory wetting.

Once a specimen was returned to the permeameter, the standpipe was replaced and again filled with de-ionized, de-aired water. A Marriott bottle was then connected to the standpipe system to ensure a constant hydraulic head above the specimen. The ball valve was then opened, allowing water to flow through the specimen and out the permeameter into a graduated flask placed at the exit point.

After the flow rate appeared to stabilize, a stop watch was used to measure the time required to collect 50 or 100 mL increments of water through a total volume of 600 mL. Increments of 100 mL were measured for specimens exhibiting higher hydraulic conductivity to facilitate more accurate time records in those tests. If 600 mL could not be collected from a given specimen within a 2-hour period, the 20-in. standpipe was removed and replaced with the 60-in. standpipe as displayed in Figure 3-8. A Marriott bottle configuration was again used to maintain constant hydraulic head in this testing.

Hydraulic conductivity was then computed using Darcy's law of flow through a porous medium shown in Equation 3-1:

$$k = \frac{QL}{Ah} \tag{3-1}$$

where k = hydraulic conductivity, ft/day

Q = discharge volume, ft^3/day

L = specimen length, ft

A = cross-sectional area, ft^2

h = hydraulic head, ft

Figure 3-8: Permeameter with Marriott bottle configuration.

The hydraulic conductivity values computed from each set of readings were averaged for each specimen. Oven-dry specimen weights were then used to compute dry densities for the tested specimens.

3.6 Statistical Analyses

Following completion of the experimental work, stepwise multivariable regression analyses were performed to investigate relationships between hydraulic conductivity and several material properties, including soil gradation and classification, fineness modulus, SG, cement content, porosity, compaction method, dry density, and 7-day UCS for each specimen. Soil gradation characteristics gathered for each specimen include the particle sizes corresponding to

percent passing values of 10, 30, and 60 percent, as well as the percentages of material retained on the No. 50, 100, and 200 sieves.

Analysis was performed using a stepwise regression in which all previously listed material properties, together with the associated two-way interactions, were initially included as independent variables for predicting hydraulic conductivity. Specifically, soil gradation, fineness modulus, SG, cement content, porosity, dry density, and 7-day UCS were treated as continuous variables, while soil classification and compaction method were treated as categorical variables. A full regression model was initially fit to the data, and the level of significance, or *p*-value, was computed for each variable. Variables having a *p*-value greater than 0.15 were then excluded from the data set and a reduced model fit to the data (*31*). This process was repeated until all variables included in the reduced model had *p*-values less than or equal to 0.15. To ensure accuracy and validity, a random-number dummy variable was also included among the independent variables in the multivariate regression. During model development, selection of the dummy variable as an independent variable signaled over-fitting of the model, and that model was then disregarded (*33*). Once a given regression model was developed, a coefficient of determination, or R^2 value, was computed. The R^2 value reflects the percentage of variation in the dependent variable that can be explained by variation in the independent variables included in the regression model, where an R^2 value of 1.0 represents a perfect model (*32*).

3.7 Summary

Each soil or aggregate type was subjected to several material characterization tests for soil classifications by the USCS and the AASHTO systems. Moisture-density curves were then developed in order to determine the OMC and MDD for each soil or aggregate type in the

untreated condition. The standard Proctor method was used for the materials from Montana and Utah, and the modified Proctor method was used for the materials from Alaska, Minnesota, and Texas.

UCS testing was performed in order to determine cement concentrations generally corresponding to target 7-day UCS values of 200, 400, and 600 psi, with selections made so that the difference between low and medium levels of cement was equal to the difference between medium and high levels of cement in each case. These three levels of cement treatment represent low, medium, and high concentrations typical of values utilized in construction projects nationwide.

After being cured for 28 days at 100 percent relative humidity, the prepared specimens were subjected to frost conditioning comprised of a sustained freeze, in which a thermal gradient was imposed over the length of the specimen, and a rapid freeze, in which the entire specimen was completely frozen. The hydraulic conductivity of each specimen was then measured using a fixed-head permeameter. Multivariable regression analyses were then performed to investigate relationships between hydraulic conductivity and several material properties, including soil gradation and classification, fineness modulus, SG, cement content, porosity, compaction method, dry density, and 7-day UCS for each specimen.

4 RESULTS

4.1 Overview

This chapter presents the results obtained from material characterization testing, moisture-density investigations, cement concentration determinations, hydraulic conductivity testing, and statistical analyses. Selected raw data are presented in Appendix A.

4.2 Material Characterization

The soil classifications obtained with USCS and AASHTO methods are presented in Table 4-1. With the AASHTO method, limited variation in soil types was recorded, as only three different AASHTO classifications were identified; however, with the USCS method, five different classifications were determined.

Table 4-1: Material Classifications

Material	USCS	AASHTO
Alaska-Dalton	Well-graded gravel with sand (GW)	A-2-4
Alaska-Elliott	Poorly-graded gravel with silt and sand (GP-GM)	A-1-a
Minnesota	Poorly-graded sand (SP)	A-1-a
Montana	Silt with sand (ML)	A-4
Texas	Poorly-graded sand with gravel (SP)	A-1-a
Utah	Silty sand (SM)	A-2-4

4.3 Moisture-Density Relationships

Values for OMC and MDD were determined from the respective moisture-density curves developed for each material and are given in Table 4-2. The lower OMC and higher MDD values are associated with aggregate base materials, while the higher OMC and lower MDD values are associated with soils.

Table 4-2: OMC and MDD Values

Material	OMC (%)	MDD (pcf)
Alaska-Dalton	4.4	145.6
Alaska-Elliott	5.3	137.3
Minnesota	3.9	131.8
Montana	20.1	101.2
Texas	5.3	146.6
Utah	12.2	120.4

4.4 Cement Concentrations

Table 4-3 displays the cement contents corresponding to low, medium, and high target 7-day UCS values for each material evaluated in this research. The measured average 7-day UCS values for each material at each of the listed cement concentrations are also provided in Table 4-3. All of the aggregate base materials achieved satisfactory strengths with less than 2 percent cement content; however, the Montana and Utah soils required higher cement concentrations.

Table 4-3: Results of 7-day UCS Testing

Material	Target Strength (psi)	Cement Concentration (%)	7-day UCS (psi)
Alaska-Elliott	Low	1.0	265
	Medium	1.5	414
	High	2.0	527
Alaska-Dalton	Low	0.5	230
	Medium	1.0	328
	High	1.5	445
Minnesota	Low	1.0	154
	Medium	1.5	258
	High	2.0	302
Montana	Low	2.0	17
	Medium	3.5	159
	High	5.0	471
Texas	Low	0.5	239
	Medium	1.0	499
	High	1.5	610
Utah	Low	2.0	155
	Medium	8.0	408
	High	14.0	607

4.5 Hydraulic Conductivity Testing

Hydraulic conductivity testing was performed on each cement-treated sample following frost conditioning. Table 4-4 displays the average value of hydraulic conductivity measured for each material treated at each cement content. Due to excessive deterioration, primarily in the form of cracking, the hydraulic conductivity of the Utah samples with a low cement concentration level could not be measured.

Table 4-4: Results of Hydraulic Conductivity Testing

Material	Cement Concentration Level	Hydraulic Conductivity (ft/day)
Alaska-Elliott	Low	66.50
	Medium	67.80
	High	73.50
Alaska-Dalton	Low	13.90
	Medium	10.90
	High	9.80
Minnesota	Low	8.10
	Medium	1.50
	High	0.52
Montana	Low	42.10
	Medium	0.28
	High	0.11
Texas	Low	0.34
	Medium	13.50
	High	3.80
Utah	Low	-
	Medium	0.84
	High	0.08

Figures 4-1 through 4-6 show average measured hydraulic conductivity values for the Alaska-Dalton, Alaska-Elliott, Minnesota, Montana, Texas, and Utah materials for each cement concentration level. The Alaska-Elliott, Minnesota, Montana, and Utah materials exhibit decreasing hydraulic conductivity with increasing UCS, the Texas material exhibits increasing hydraulic conductivity with increasing strength from the low to medium cement concentration levels but decreasing hydraulic conductivity from the medium to high cement concentration levels, and the Alaska-Dalton material exhibits increasing hydraulic conductivity with increasing strength.

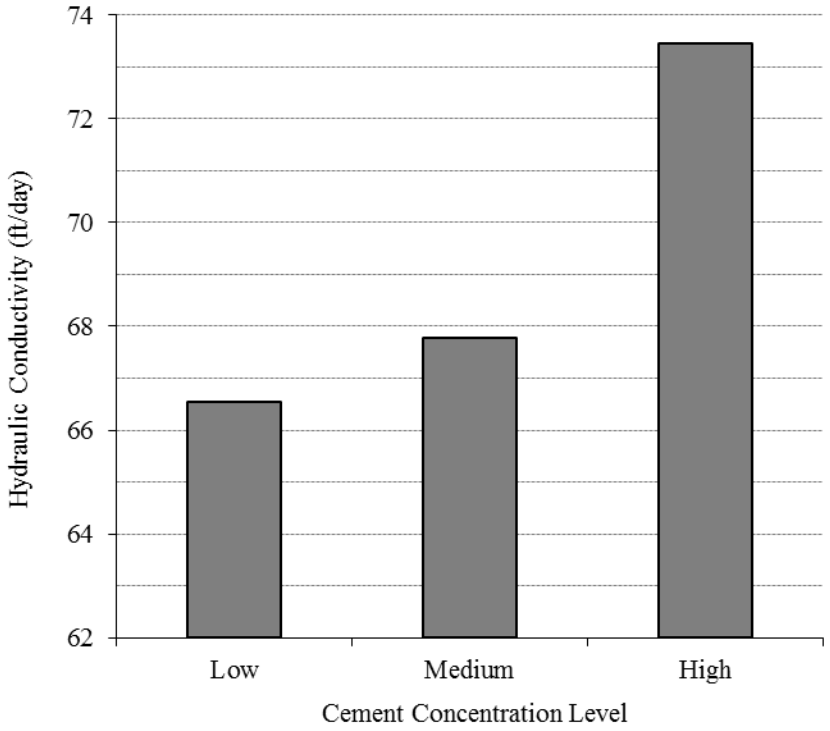

Figure 4-1: Average hydraulic conductivity values for Alaska-Dalton material.

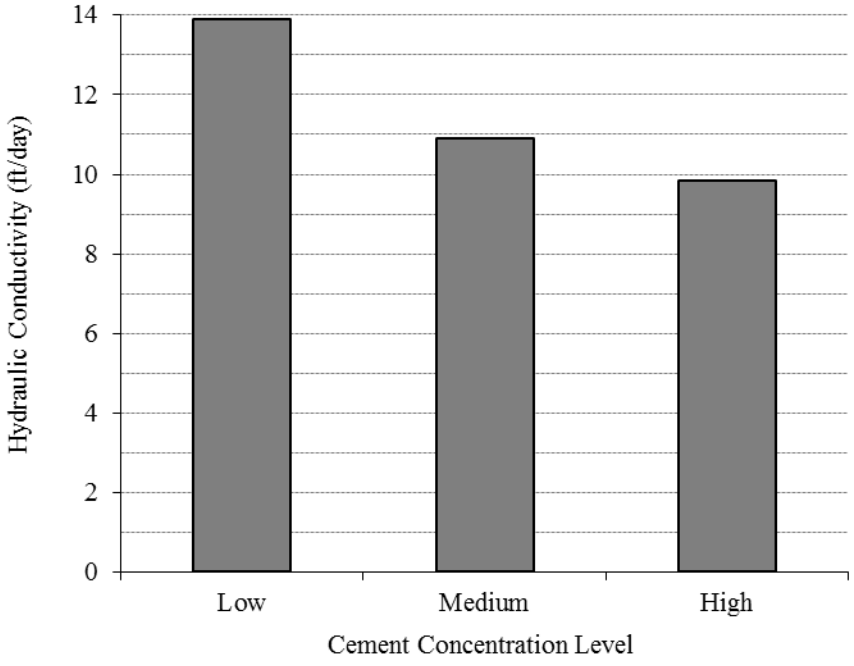

Figure 4-2: Average hydraulic conductivity values for Alaska-Elliott material.

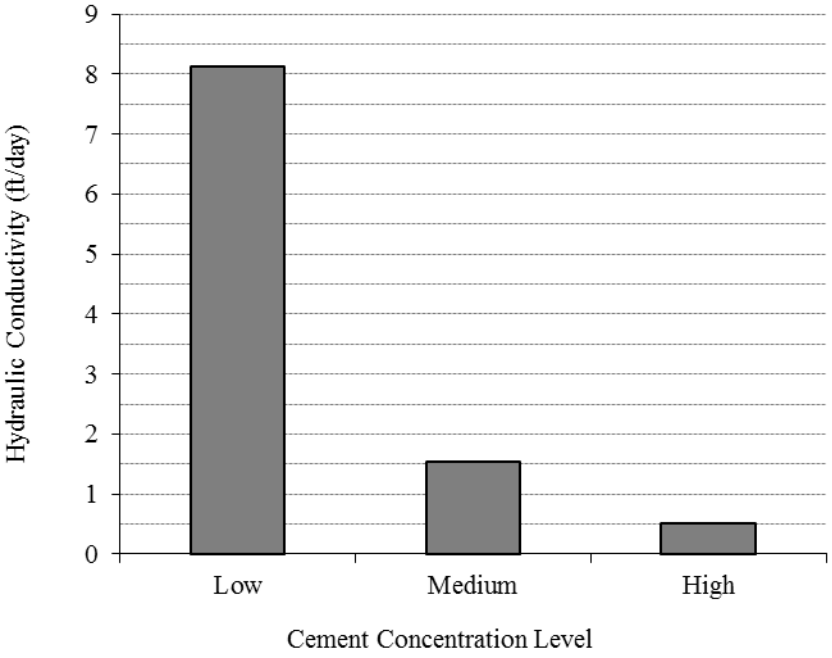

Figure 4-3: Average hydraulic conductivity values for Minnesota material.

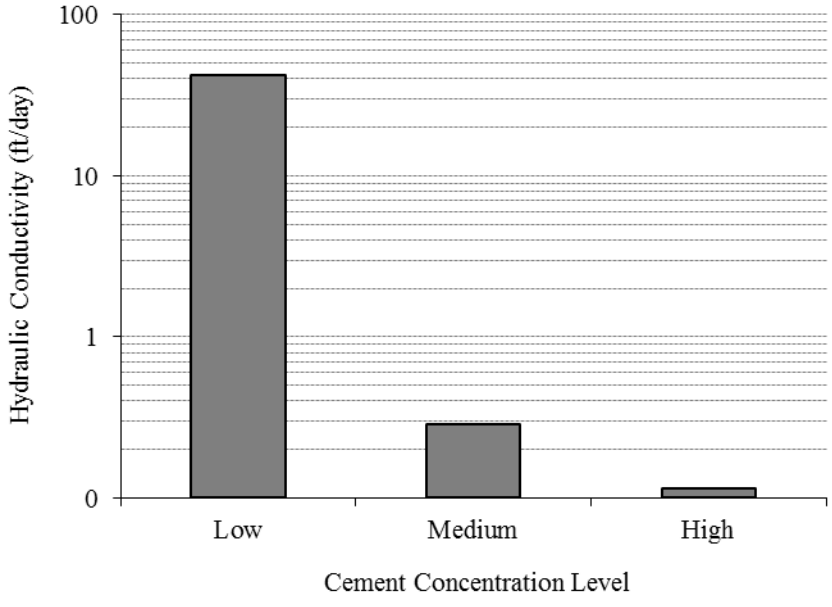

Figure 4-4: Average hydraulic conductivity values for Montana material.

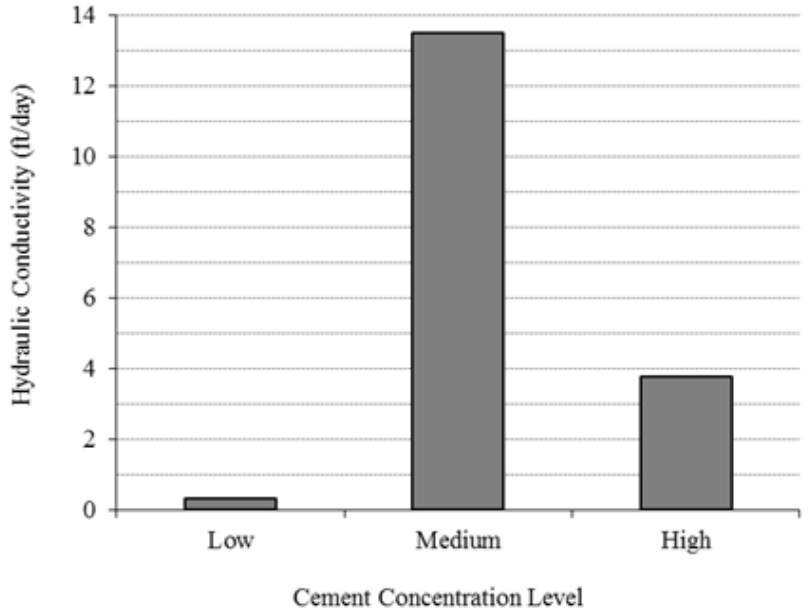

Figure 4-5: Average hydraulic conductivity values for Texas material.

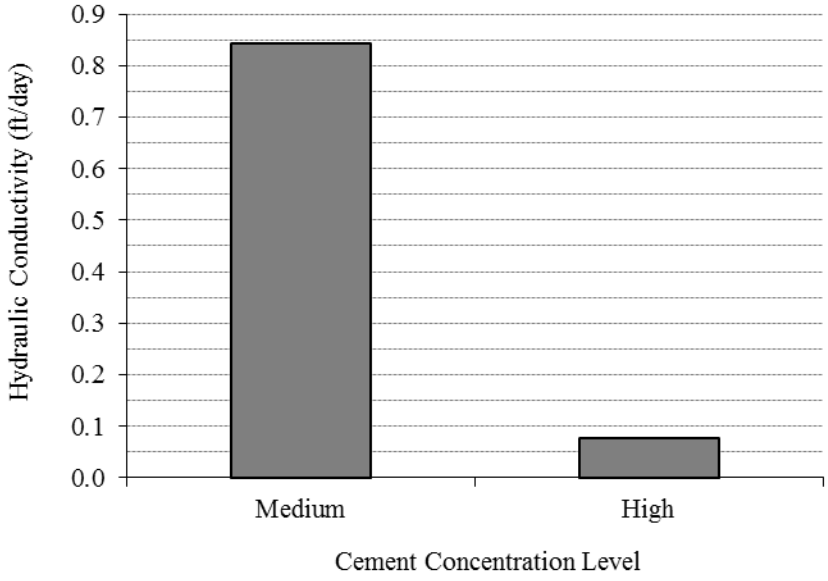

Figure 4-6: Average hydraulic conductivity values for Utah material.

4.6 Statistical Analyses

Because the hydraulic conductivity values varied by over an order of magnitude from the largest to the smallest measurements, a logarithmic transformation was applied to all the hydraulic conductivity values before statistical analyses were performed. Logarithmic transformations were also considered for all other factors available for inclusion in the statistical models. However, because these additional transformations increased the complexity of the models and increased the R^2 value by less than 5.0 percent, only the hydraulic conductivity values were transformed. Four different regression models were prepared, including a six-parameter model, a four-parameter model, a USCS model, and an AASHTO-classification model. Appendices B through E present plots showing the relationships between hydraulic conductivity and individual independent variables included in the regression equations developed for each of the models. Each plot shows values of hydraulic conductivity computed from the models at the minimum, average, and maximum values of the independent variables and at two standard deviations above and below the average.

The four regression models are given in Equations 4-1 to 4-4, corresponding to the six-parameter, four-parameter, USCS, and AASHTO-classification model, respectively:

$$\begin{aligned} Log\ k = {} & 2.5504 - 0.004733(P_{50})(UCS) + 1677.5(D_{10})(D_{30}) \\ & - 822.64(D_{10})(P_{50}) + 0.048175(D_{30})(UCS) \\ & - 0.11511(D_{30})(\gamma_D) - 0.001981(SG)(UCS) \end{aligned} \quad (4\text{-}1)$$

$$\begin{aligned} Log\ k = {} & 2.3865 - 0.010146(P_{50})(UCS) + 1619.5(D_{10})(D_{30}) \\ & - 2137.4(D_{10})(P_{50}) + 0.010409(D_{30})(UCS) \end{aligned} \quad (4\text{-}2)$$

$$\begin{aligned} k = {} & 184.91 - 137.94(P_{100}) - 11.786(LnUCS) + 16.134(D_{10})(UCS) \\ & + 1089.9(D_{60})(SG) - 19.094(D_{60})(\gamma_D) \\ & + 12.822(LnP_{100})(LnUCS) + U \end{aligned} \quad (4\text{-}3)$$

$$Log\ k = 2.3297 - 0.13653(C) - 6.2830(D_{30}) + 0.40853(P_{50}) - 0.0065387(UCS) - 0.0038082(P_{50})(UCS) + 17.148(D_{30})(C) + A \quad (4\text{-}4)$$

where k = hydraulic conductivity, ft/day

P_{50} = percentage of the material passing the No. 50 sieve

UCS = unconfined compressive strength, psi

D_{10} = particle-size diameter at which 10 percent is finer, in.

D_{30} = particle-size diameter at which 30 percent is finer, in.

γ_D = dry density, lb/ft^3

SG = apparent specific gravity of the soil particles

P_{100} = percentage of the material passing the No. 100 sieve

D_{60} = particle-size diameter at which 60 percent is finer, in.

U = USCS reference value from Table 4-5

C = cement content, % by weight of dry aggregate

A = AASHTO reference value from Table 4-6

Tables 4-5 and 4-6 contain reference values to be used in the USCS and AASHTO-classification models, respectively; in both cases, different reference values are given for different soil classifications. This research included five different USCS classifications and three different AASHTO classifications; all other USCS and AASHTO classifications are outside the scope of this research. The R^2 values computed for the six-parameter, four-parameter, USCS, and AASHTO-classification models are 0.795, 0.767, 0.930, and 0.782, respectively.

Table 4-5: Reference Values for USCS Model

Classification	Coefficient
GP-GM	-50.392
GW	-128.80
ML	-62.353
SM	14.139
SP	0.00

Table 4-6: Reference Values for AASHTO-Classification Model

Classification	Coefficient
A-1-a	0.095137
A-2-4	2.7345
A-4	0.00

Graphical comparisons of estimated and measured hydraulic conductivities are provided in Figures 4-7 to 4-10, corresponding to Equations 4-1 to 4-4, respectively. A line of equality is provided in each figure as a reference.

Values of hydraulic conductivity computed using these equations will be more reliable when more input parameters are available. However, because certain parameters such as SG are less commonly available, use of the four-parameter model instead of the six-parameter model may be warranted in some cases. While both the four- and six-parameter models can be used for any soil or aggregate for which the required input parameters are known, the USCS and AASHTO-classification models are valid only for the selected soil classifications listed in Tables 4-5 and 4-6. When applicable, use of the USCS model is recommended because it has the highest R^2 value.

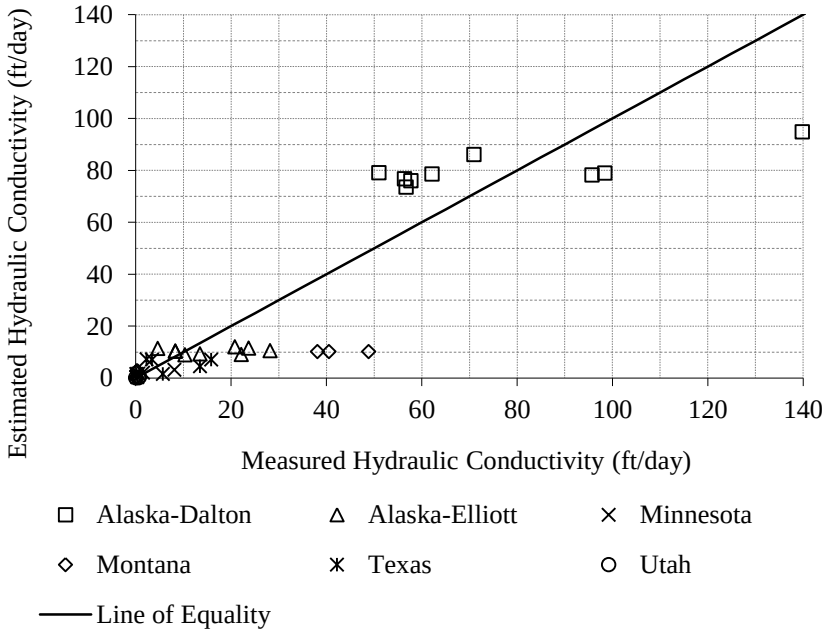

Figure 4-7: Comparison of estimated and measured hydraulic conductivities for six-parameter model.

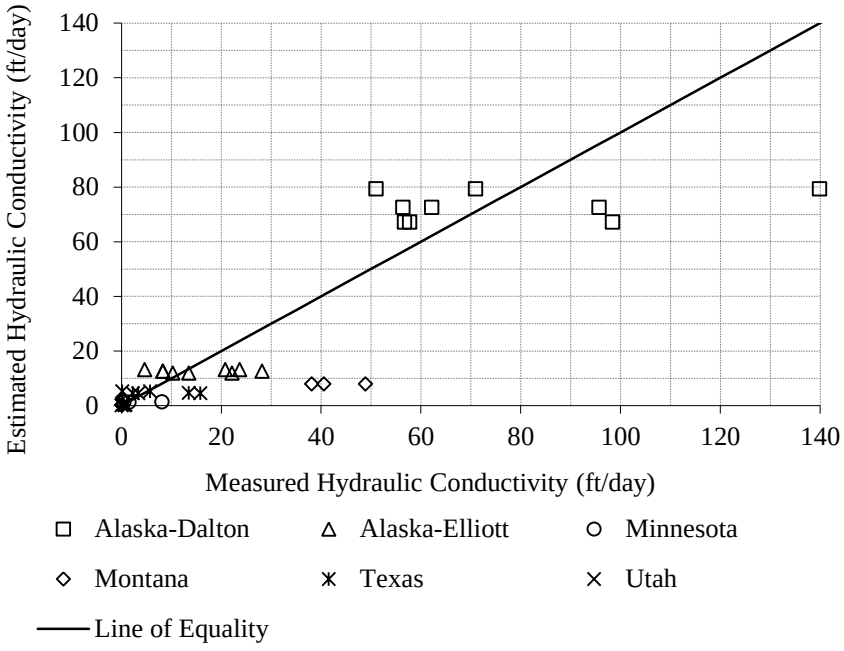

Figure 4-8: Comparison of estimated and measured hydraulic conductivities for four-parameter model.

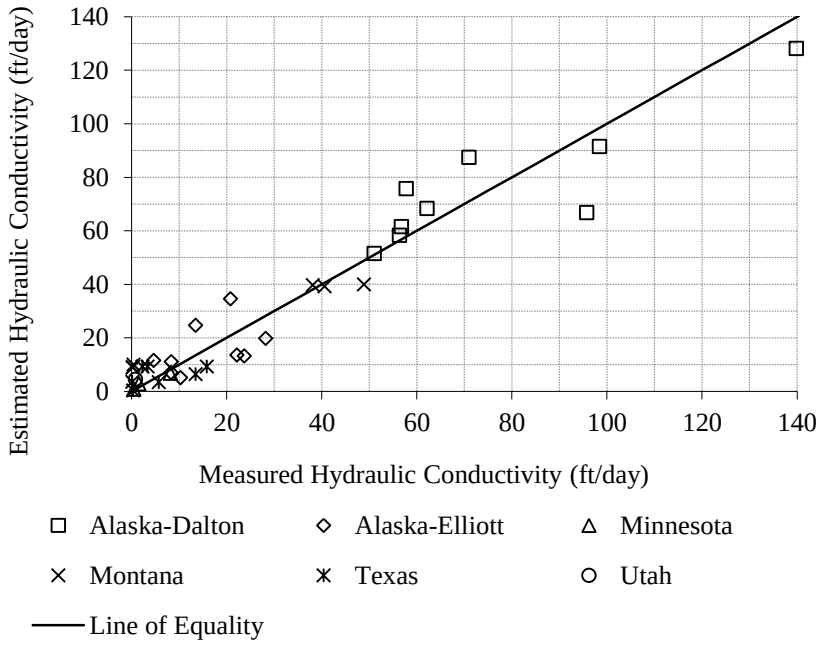

Figure 4-9: Comparison of estimated and measured hydraulic conductivities for USCS model.

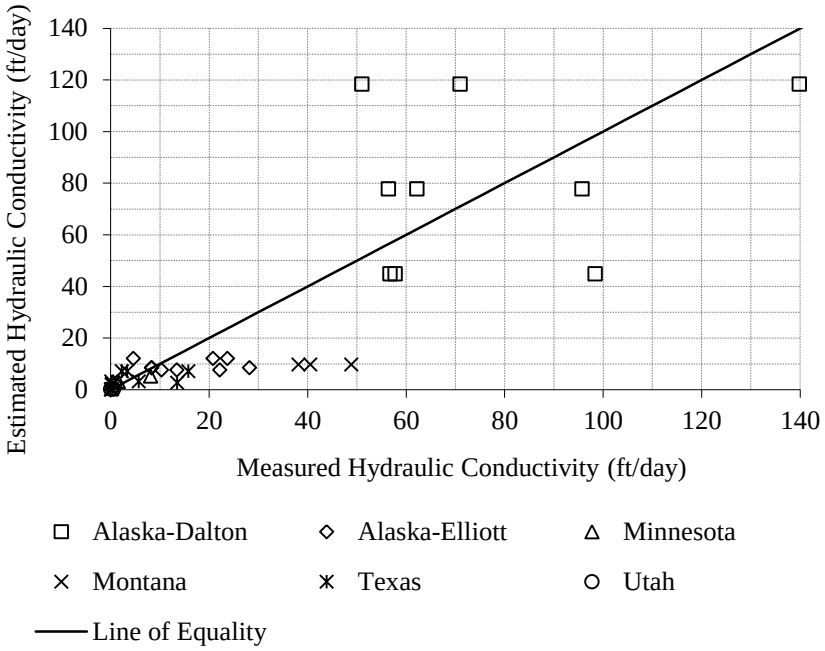

Figure 4-10: Comparison of estimated and measured hydraulic conductivities for AASHTO-classification model.

4.7 Summary

The OMC values determined for the materials evaluated in this research range from 3.9 percent for the Minnesota material to 20.1 percent for the Montana material, while MDD values range from 101.2 pcf for the Montana material to 146.6 pcf for the Texas material. Lower OMC and higher MDD values are associated with aggregate base materials, while higher OMC and lower MDD values were associated with soils. The cement contents corresponding to low, medium, and high target 7-day UCS values were achieved with less than 2 percent cement for all of the aggregate base materials evaluated in this research; however, the Montana and Utah soils required cement concentrations as high as 5.0 and 14.0 percent, respectively.

Hydraulic conductivities measured on the frost-conditioned, cement-treated soils and aggregates tested in this study range from 0.08 to 73.5 ft/day. The Alaska-Elliott, Minnesota, Montana, and Utah materials exhibit decreasing hydraulic conductivity with increasing UCS, the Texas material exhibits increasing hydraulic conductivity with increasing strength from the low to medium cement concentration levels but decreasing hydraulic conductivity from the medium to high cement concentration levels, and the Alaska-Dalton material exhibits increasing hydraulic conductivity with increasing strength.

A stepwise regression analysis of the data set produced four models to estimate hydraulic conductivity of cement-treated soils. The R^2 values computed for the six-parameter, four-parameter, USCS, and AASHTO-classification models are 0.795, 0.767, 0.930, and 0.782, respectively. Values of hydraulic conductivity computed using these equations will be more reliable when more input parameters are available. However, because certain parameters such as SG are less commonly available, use of the four-parameter model instead of the six-parameter model may be warranted in some cases. While both the four- and six-parameter models can be

used for any soil or aggregate for which the required input parameters are known, the USCS and AASHTO-classification models are valid only for the selected soil classifications listed in Tables 4-5 and 4-6. When applicable, use of the USCS model is recommended because it has the highest R^2 value.

5 CONCLUSION

5.1 Summary

Water movement through soils and aggregates comprising pavement structures can cause material degradation, resulting in reduced bearing capacity and accelerated development of distress. Moisture infiltration results in frost damage manifested as frost heave and surface roughness during winter and thaw-weakening during spring. Improvements in the strength and durability of frost-susceptible soils and aggregates can be achieved through chemical stabilization using portland cement, where the efficacy of cement stabilization for improving durability depends on the degree to which hydraulic conductivity is reduced.

Estimating hydraulic conductivity is commonly accomplished through the use of Moulton's empirical equation, which uses basic soil properties to estimate hydraulic conductivity. However, the hydraulic conductivity estimation does not consider the detrimental effects of freezing or the benefits of cement stabilization. The purpose of this research was to derive new equations relating hydraulic conductivity after freezing to specific material properties of cement-treated soils and aggregates stabilized with different concentrations of cement.

This research included material samples from two locations in Alaska and from single locations in Minnesota, Montana, Texas, and Utah, for a total of six material samples. Each soil or aggregate type was subjected to several material characterization tests for soil classifications by the USCS and the AASHTO systems. Moisture-density curves were then developed, and

UCS testing was performed in order to determine cement concentrations generally corresponding to low, medium, and high 7-day UCS values of 200, 400, and 600 psi, respectively. After being cured for 28 days at 100 percent relative humidity, the prepared specimens were subjected to frost conditioning and hydraulic conductivity testing, which was performed using a fixed-head permeameter. Multivariable regression analyses were then performed to investigate relationships between hydraulic conductivity and several material properties, including soil gradation and classification, fineness modulus, SG, cement content, porosity, compaction method, dry density, and 7-day UCS for each specimen.

5.2 Findings

The cement contents corresponding to low, medium, and high target 7-day UCS values were achieved with less than 2 percent cement for all of the aggregate base materials evaluated in this research; however, the Montana and Utah soils required cement concentrations as high as 5.0 and 14.0 percent, respectively. The Alaska-Elliott, Minnesota, Montana, and Utah materials exhibit decreasing hydraulic conductivity with increasing UCS, the Texas material exhibits increasing hydraulic conductivity with increasing strength from the low to medium cement concentration levels but decreasing hydraulic conductivity from the medium to high cement concentration levels, and the Alaska-Dalton material exhibits increasing hydraulic conductivity with increasing strength.

A stepwise regression analysis of the data set produced four models to estimate hydraulic conductivity of cement-treated soils. The R^2 values computed for the six-parameter, four-parameter, USCS, and AASHTO-classification models are 0.795, 0.767, 0.930, and 0.782, respectively. While both the four- and six-parameter models can be used for any soil or

aggregate, the USCS and AASHTO-classification models are valid only for the selected soil classifications listed in Tables 4-5 and 4-6.

5.3 Recommendations

Values of hydraulic conductivity computed using these equations will be more reliable when more input parameters are available. When applicable, use of the USCS model is recommended because it has the highest R^2 value. Further research is recommended to investigate the effects of cement on hydraulic conductivity for USCS and AASHTO soil types not covered in this research. This work will particularly benefit pavement and materials engineers working in regions in which frost action is prevalent.

REFERENCES

1. Frietag, D. R., and T. McFadden. *Introduction to Cold Regions Engineering*. ASCE Press, New York, NY, 1997.

2. Jessberger, H. L., and D. L. Carbee. Influence of Frost Action on the Bearing Capacity of Soils. In *Highway Research Board Bulletin, No. 304*, HRB, National Research Council, Washington, DC, 1970, pp. 14-26.

3. Jones, R. H. Frost Heave of Roads. *Quarterly Journal of Engineering Geology*, Vol. 13, No. 2, 1980, pp. 77-86.

4. Chamberlain, E. J. *Frost Susceptibility of Soil and Review of Index Tests*. Monograph 81-2. US Army Cold Regions Research and Engineering Laboratory, Hanover, NH, 1981.

5. Guthrie, W. S. Determining Aggregate Frost Susceptibility with the Tube Suction Test. In *Proceedings of the American Society of Civil Engineers Eleventh International Conference: Cold Regions Engineering: Cold Regions Impacts on Transportation and Infrastructure*, Anchorage, AK, May 2002, pp. 663-674.

6. Janoo, V. C. Performance of Base/Subbase Materials under Frost Action. In *Proceedings of the American Society of Civil Engineers Eleventh International Conference: Cold Regions Engineering: Cold Regions Impacts on Transportation and Infrastructure*, Anchorage, AK, May 2002, pp. 299-310.

7. Lay, R. *Development of a Frost Heave Test Apparatus*. M.S. thesis. Department of Civil and Environmental Engineering, Brigham Young University, Provo, UT, December 2005.

8. State-of-the-Art Report on Soil Cement. *ACI Materials Journal*, Vol. 87, No. 4, July/August 1990, pp. 395-417.

9. Eaton, R. A., A. G. Hansom, M. A. Kestler, A. Hall, and H. J. Miller. Spring Thaw Predictor and Development of Real Time Spring Load Restrictions. In *Proceedings of the American Society of Civil Engineers Fourteenth International Conference: Cold Regions Engineering: Cold Regions Impacts on Research, Design, and Construction*. CD-ROM. Duluth, MN, 2009.

10. Othman, M. A., C. H. Benson, E. J. Chamberlain, and T. F. Zimmie. State-of-the-Art: Laboratory Testing to Evaluate Changes in Hydraulic Conductivity of Compacted Clays Caused by Freeze-Thaw. In *Hydraulic Conductivity and Waste Contaminant Transport in Soil, ASTM STP 1142*, D. E. Daniel and S. J. Trautwein, Eds., American Society for Testing and Materials, Philadelphia, PA, 1994, pp. 227-254.

11. O'Neill, K., and R. D. Miller. Exploration of a Rigid Ice Model of Frost Heave. *Water Resources Research*, Vol. 21, No. 3, March 1985, pp. 281-296.

12. Huang, Y. H. *Pavement Analysis and Design*, Second Edition. Prentice Hall, Upper Saddle River, NJ, 2004.

13. Crook, A. L. *Assessment of the Tube Suction Test for Identifying Non-Frost Susceptible Soils Stabilized with Cement*. M.S. thesis. Department of Civil and Environmental Engineering, Brigham Young University, Provo, UT, December 2006.

14. Hanks, R. J., and G. L. Ashcroft. *Applied Soil Physics*. Springer-Verlag, New York, NY, 1980.

15. Taber, S. Freezing and Thawing of Soils as Factors in the Destruction of Road Pavements. *Public Roads*, Vol. 11, No. 6, 1930, pp. 113-132.

16. Miller, R. D. Freezing and Heaving of Saturated and Unsaturated Soils. In *Highway Research Record, No. 393*, HRB, National Research Council, Washington, DC, 1972, pp. 1-11.

17. Loch, J. P. G. Influence of the Heat Extraction Rate on the Ice Segregation Rate of Soils. *Frost i Jord*, No. 20, 1979, pp. 19-30.

18. Konrad, J. M., and N. R. Morgenstern. A Mechanistic Theory of Ice Lens Formation in Fine-Grained Soils. *Canadian Geotechnical Journal*, Vol. 17, No. 4, National Research Council of Canada, Ottawa, Ontario, Canada, 1980, pp. 473-486.

19. Guthrie, W. S., and Å. Hermansson. Frost Heave and Water Uptake Relations in Variably Saturated Aggregate Base Materials. In *Transportation Research Record: Journal of the Transportation Research Board, No. 1821*, Transportation Research Board of the National Academies, Washington, DC, 2003, pp. 13-19.

20. Andersland, O. B., and D. M. Anderson. *Geotechnical Engineering for Cold Regions*. McGraw-Hill Book Company, New York, NY, 1978.

21. Penner, E. Ground Freezing and Frost Heaving. February 1962. http://irc.nrc-cnrc.gc.ca/pubs/cbd/cbd026_e.html. Accessed Jun. 26, 2008.

22. Johnson, G. H. *Permafrost: Engineering Design and Construction*. John Wiley and Sons, Toronto, Ontario, Canada, 1981.

23. Andersland, O. B., and B. Ladanyi. *An Introduction to Frozen Ground Engineering*. Chapman and Hall, New York, NY, 1994.

24. Lindh, P. *Soil Stabilisation of Fine-Grained Till Soils: The Effect of Lime and Hydraulic Binders on Strength and Compaction Properties*. Licentiate thesis. Department of Geotechnical Soil Mechanics and Foundation Engineering, Lund Institute of Technology, Lund University, Sweden, 2000.

25. Guthrie, W. S., R. D. Lay, and A. J. Birdsall. Effect of Reduced Cement Contents on Frost Heave of Silty Soil: Laboratory Testing and Numerical Modeling. In *Transportation Research Board 86th Annual Meeting Compendium of Papers.* CD-ROM. Transportation Research Board, National Research Council, Washington, DC, January 2007.

26. Vervoort, R. W., and S. R. Cattle. Linking Hydraulic Conductivity and Tortuosity Parameters to Pore Space Geometry and Pore-Size Distribution. *Journal of Hydrology*, Vol. 272, No. 1-4, March 2003, pp. 36-49.

27. Kettle, R. J., and E. Y. McCabe. Mechanical Stabilization for the Control of Frost Heave. *Canadian Journal of Civil Engineering*, Vol. 12, No. 2, 1985, pp. 899-905.

28. Lofti, H., and M. W. Witczak. Dynamic Characterization of Cement-Treated Base and Subbase Materials. In *Transportation Research Record: Journal of the Transportation Research Board, No. 1031*, Transportation Research Board of the National Academies, Washington, DC, pp. 41-48.

29. Guthrie, W. S., and T. B. Young. Evaluation of Transition Cement for Stabilization of Frost-Susceptible Base Materials in Conjunction with Full-Depth Recycling in Weber Canyon, Utah. In *Proceedings of the American Society of Civil Engineers Thirteenth International Conference on Cold Regions Engineering*. CD-ROM. Orono, ME, July 2006.

30. Das, B. M. *Principles of Geotechnical Engineering*, Sixth Edition. Thomson Canada Limited, Toronto, Ontario, Canada, 2006.

31. Daniel, D. E. State-of-the-Art: Laboratory Hydraulic Conductivity Tests for Saturated Soils. *Hydraulic Conductivity and Waste Contaminant Transport in Soil, ASTM STP 1142*, D. E. Daniel and S. J. Trautwein Eds., American Society for Testing and Materials, Philadelphia, PA, 1994, pp. 30-78.

32. Ramsey, F. L., and D. W. Schafer. *The Statistical Sleuth*, Second Edition. Duxbury, Pacific Grove, CA, 2002.

APPENDIX A: MATERIAL PROPERTIES

Table A-1: Particle-Size Distribution and Specific Gravity Data

Property	Material					
	Alaska-Dalton	Alaska-Elliott	Minnesota	Montana	Texas	Utah
D_{10} (in.)	0.0215	0.0109	0.0148	0.0000935	0.00313	0.0000185
D_{30} (in.)	0.150	0.141	0.0349	0.000742	0.2170	0.000476
D_{60} (in.)	0.383	0.372	0.167	0.0726	0.00313	0.00362
P_{50} (%)	7.83	10.7	8.99	86.8	26.1	81.7
P_{100} (%)	6.00	8.24	4.36	82.0	85.5	73.0
P_{200} (%)	4.33	6.86	2.24	71.0	90.4	48.1
Fineness Modulus	5.48	5.32	4.39	0.509	3.54	0.00886
SG	3.01	2.65	2.72	2.67	2.52	2.41

Table A-2: Hydraulic Conductivity Data

Material Type	Cement Content (%)	Specimen	Dry Density (pcf)	Porosity	Hydraulic Conductivity (ft/day)
Alaska-Dalton	0.5	1	143.1	0.240	57.75
		2	145.1	0.210	56.77
		3	141.0	0.219	98.44
	1.0	1	147.9	0.204	56.40
		2	146.5	0.213	62.18
		3	146.7	0.209	95.74
	1.5	1	152.4	0.207	51.02
		2	141.9	0.228	139.88
		3	147.4	0.212	70.98
Alaska-Elliott	1.0	1	137.1	0.164	13.49
		2	138.6	0.137	22.16
		3	139.8	0.143	10.34
	1.5	1	140.5	0.153	8.31
		2	139.9	0.138	8.35
		3	138.7	0.154	28.21
	2.0	1	140.9	0.153	23.73
		2	137.9	0.150	20.84
		3	141.2	0.138	4.65
Minnesota	1.0	1	138.7	0.185	8.13
	1.5	1	139.4	0.175	1.55
	2.0	1	140.7	0.173	0.52
Montana	2.0	1	101.3	0.392	48.91
		2	101.8	0.389	40.59
		3	101.5	0.391	38.15
	3.5	1	99.8	0.401	0.40
		2	100.5	0.397	0.30
		3	100.6	0.396	0.21
	5.0	1	100.6	0.396	0.15
		2	100.2	0.399	0.11
		3	100.3	0.398	0.09
Texas	0.5	1	143.8	0.090	0.17
		2	145.7	0.084	5.74
		3	146.1	0.135	0.34
	1.0	1	145.3	0.106	13.50
	1.5	1	146.0	0.083	3.40
		2	145.3	0.083	2.29
		3	146.3	0.087	15.8
Utah	8.0	1	118.4	0.216	0.84
	14.0	1	119.8	0.207	0.62
		2	118.3	0.218	0.04

Table A-3: Strength Data

Material Type	Cement Content (%)	Specimen	7-day UCS (psi)
Alaska-Dalton	0.5	1	239
		2	199
		3	251
	1.0	1	335
		2	324
		3	325
	1.5	1	378
		2	469
		3	489
Alaska-Elliott	1.0	1	266
		2	305
		3	224
	1.5	1	339
		2	570
		3	446
		4	302
	2.0	1	518
		2	551
		3	512
Minnesota	1.0	1	135
		2	128
		3	199
	1.5	1	232
		2	243
		3	300
	2.0	1	307
		2	321
		3	279
Montana	2.0	1	23
		2	14
		3	14
	3.5	1	164
		2	138
		3	176
	5.0	1	213
		2	540
		3	660

Table A-3: (continued.)

Material Type	Cement Content (%)	Specimen	7-day UCS (psi)
Texas	0.5	1	239
	1.0	1	499
	1.5	1	610
Utah	2.0	1	73
		2	187
		3	206
	8.0	1	425
		2	395
		3	404
	14.0	1	560
		2	604
		3	658

APPENDIX B: HYDRAULIC CONDUCTIVITY RESULTS FROM SIX-PARAMETER MODEL

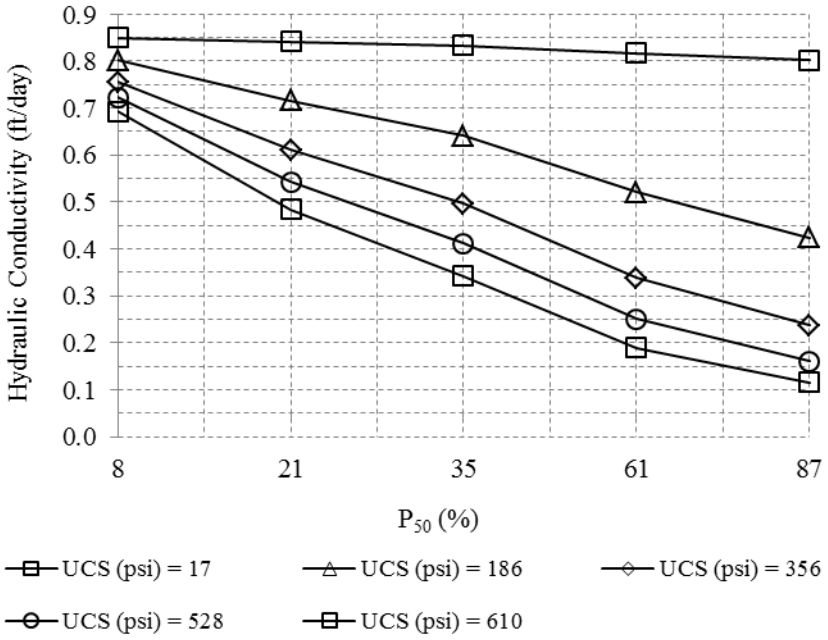

Figure B-1: Two-way interaction between P_{50} and 7-day UCS for six-parameter model.

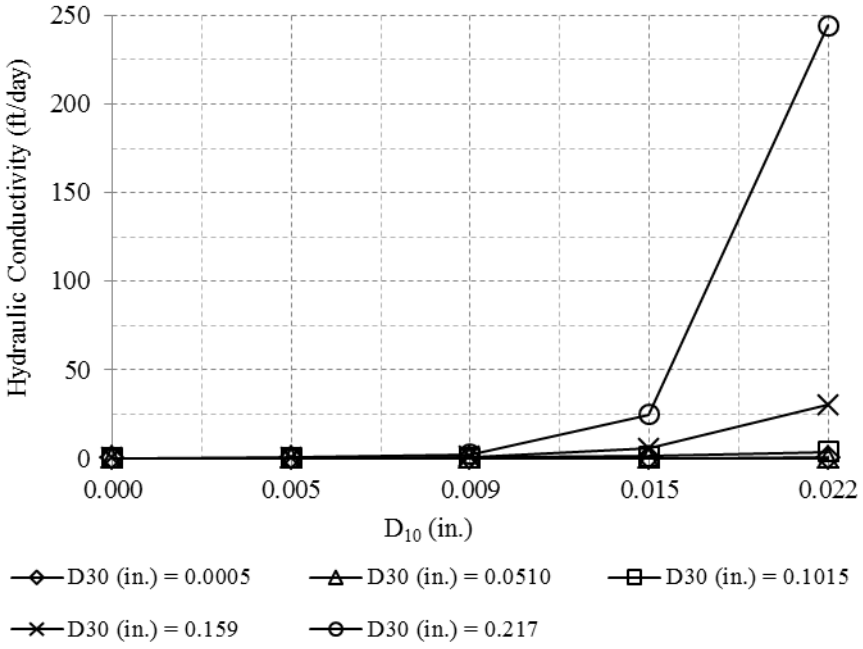

Figure B-2: Two-way interaction between D_{10} and D_{30} for six-parameter model.

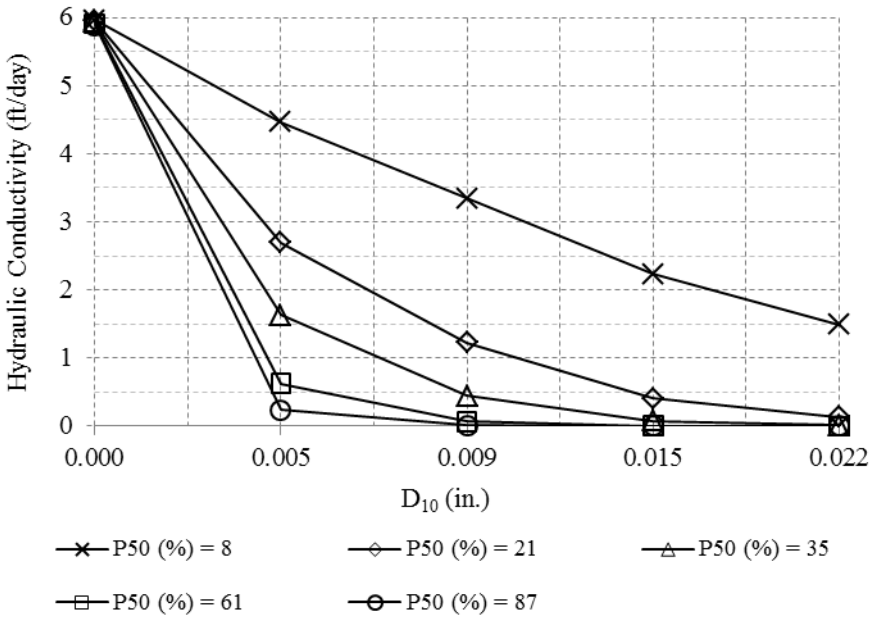

Figure B-3: Two-way interaction between D_{10} and P_{50} for six-parameter model.

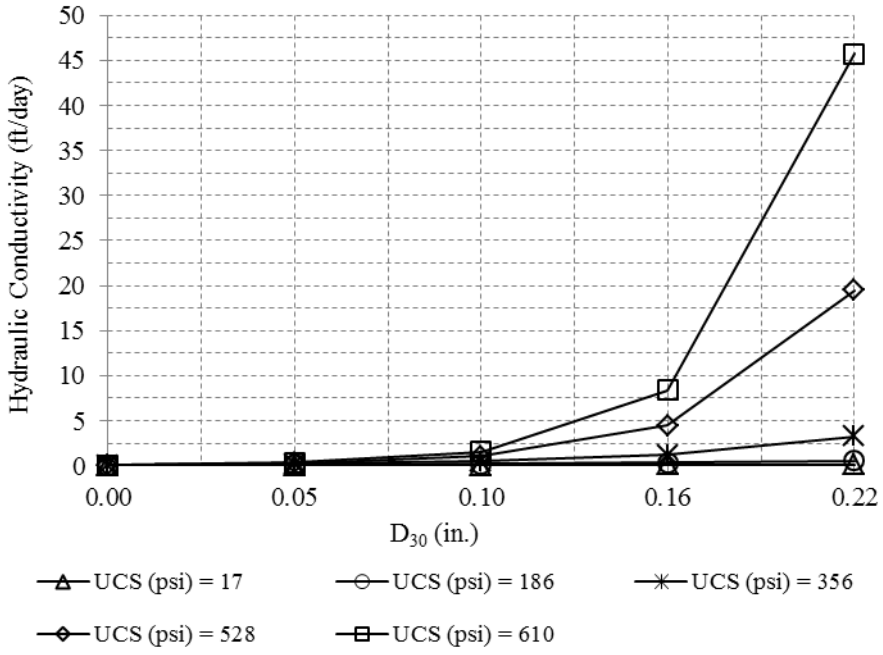

Figure B-4: Two-way interaction between D_{30} and 7-day UCS for six-parameter model.

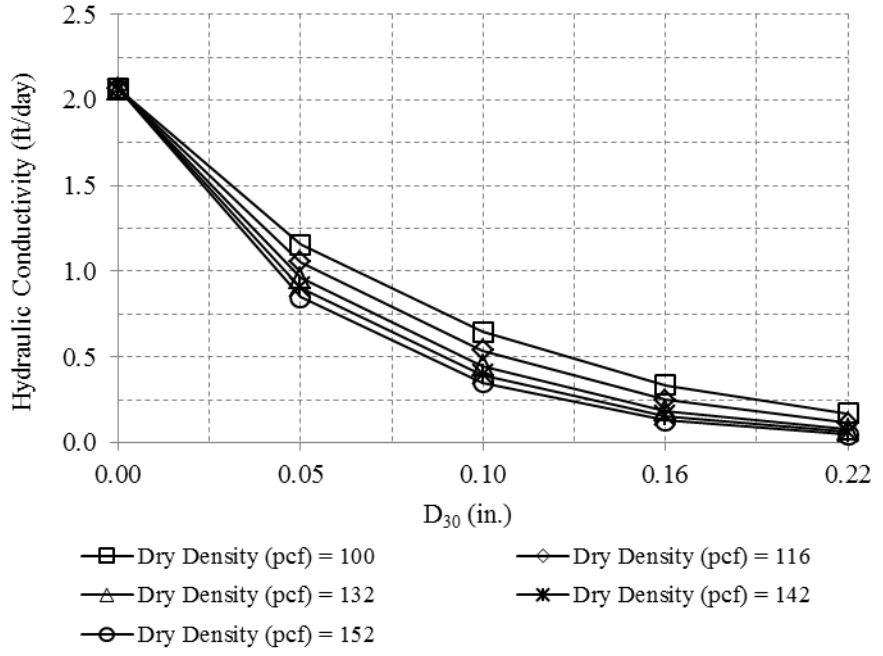

Figure B-5: Two-way interaction between D_{30} and dry density for six-parameter model.

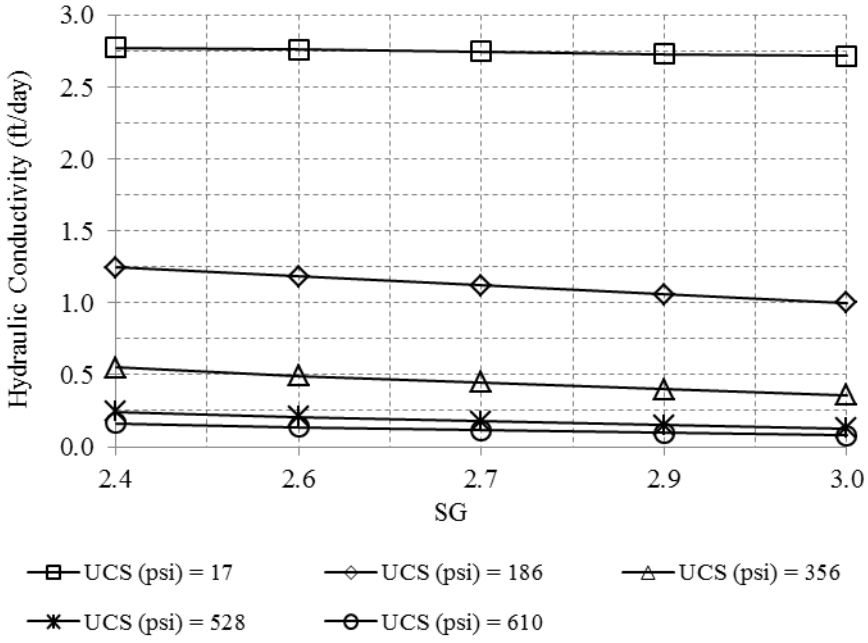

Figure B-6: Two-way interaction between SG and 7-day UCS for six-parameter model.

APPENDIX C: HYDRAULIC CONDUCTIVITY RESULTS FROM FOUR-PARAMETER MODEL

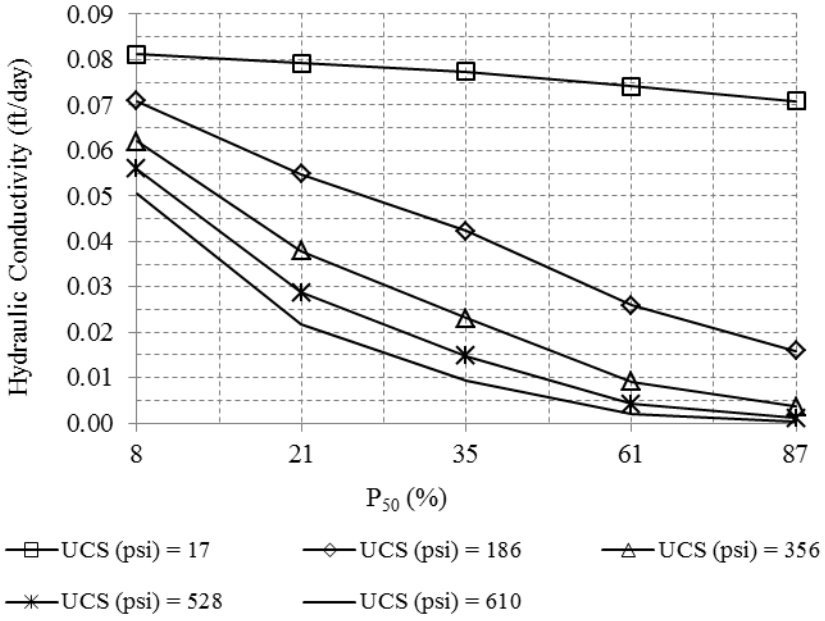

Figure C-1: Two-way interaction between P_{50} and 7-day UCS for four-parameter model.

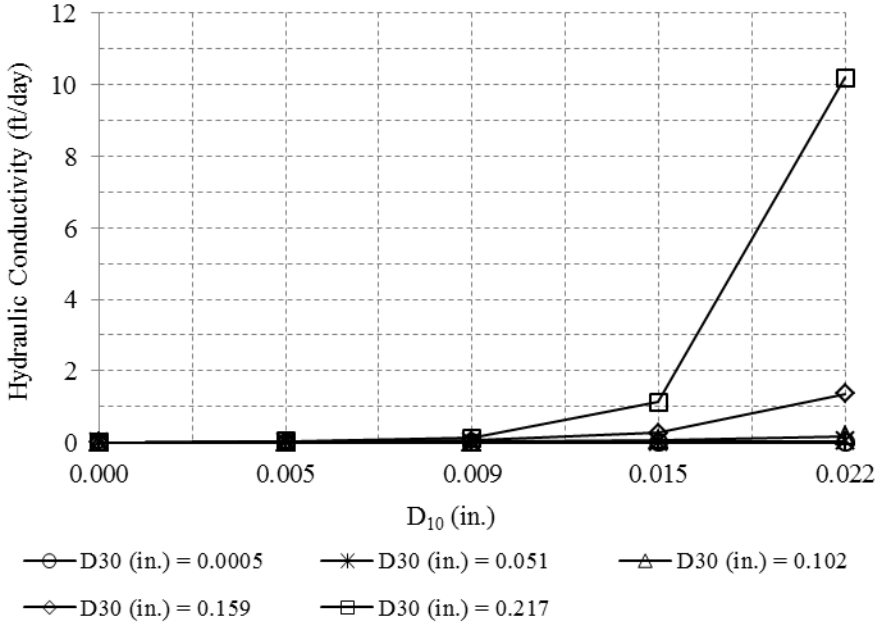

Figure C-2: Two-way interaction between D_{10} and D_{30} for four-parameter model.

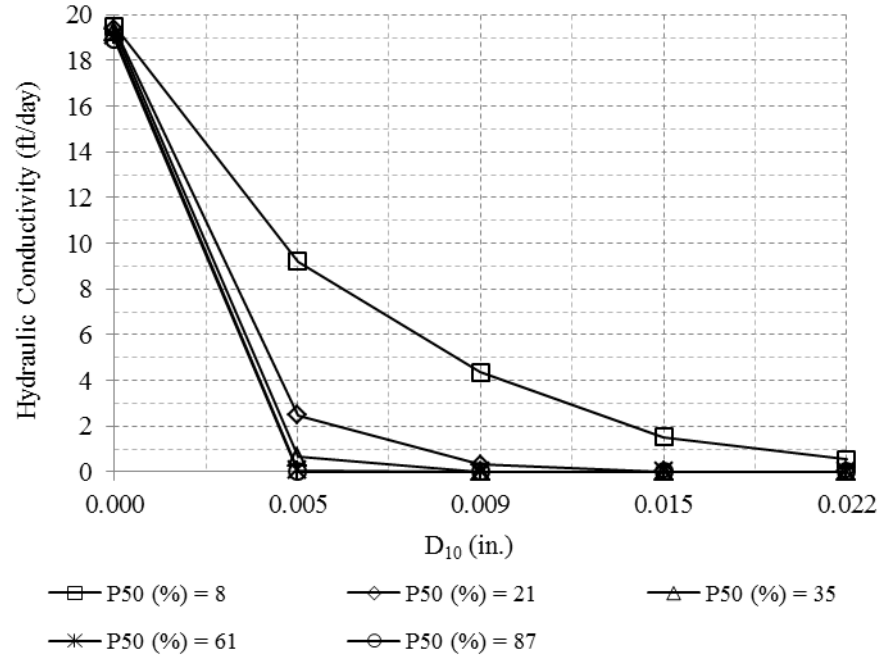

Figure C-3: Two-way interaction between D_{10} and P_{50} for four-parameter model.

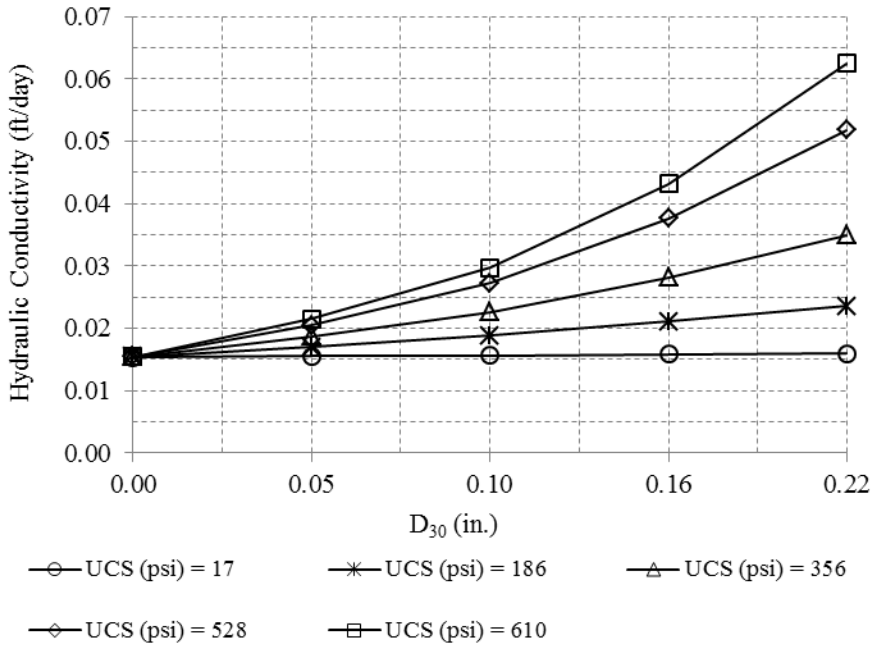

Figure C-4: Two-way interaction between D_{30} and 7-day UCS for four-parameter model

APPENDIX D: HYDRAULIC CONDUCTIVITY RESULTS FROM USCS MODEL

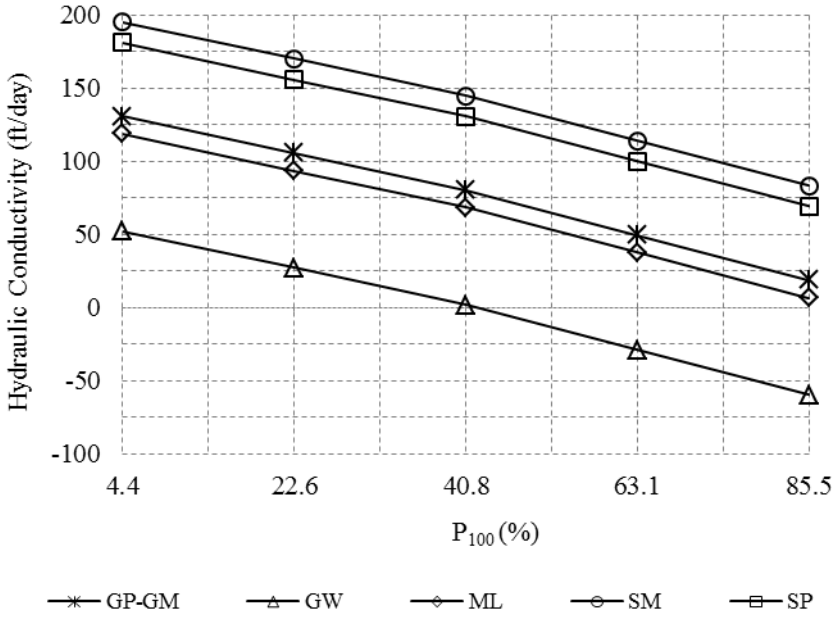

Figure D-1: Two-way interaction between P_{100} and Unified soil classification for USCS model.

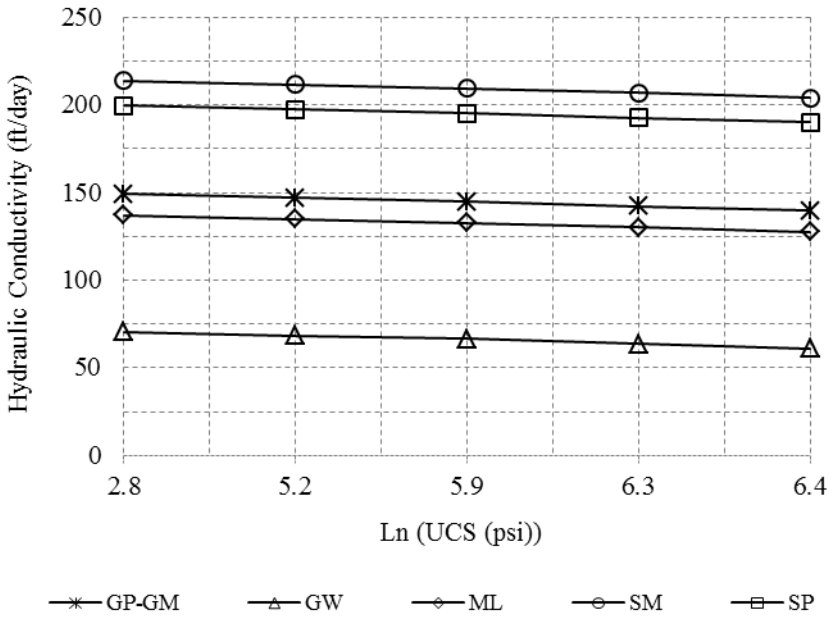

Figure D-2: Two-way interaction between Ln 7-day UCS and Unified soil classification for USCS model.

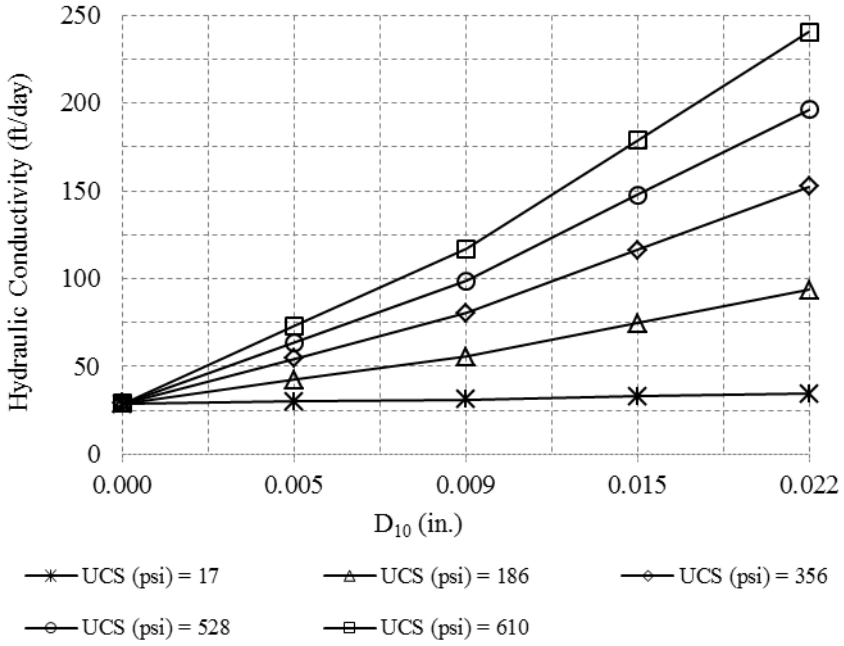

(a)

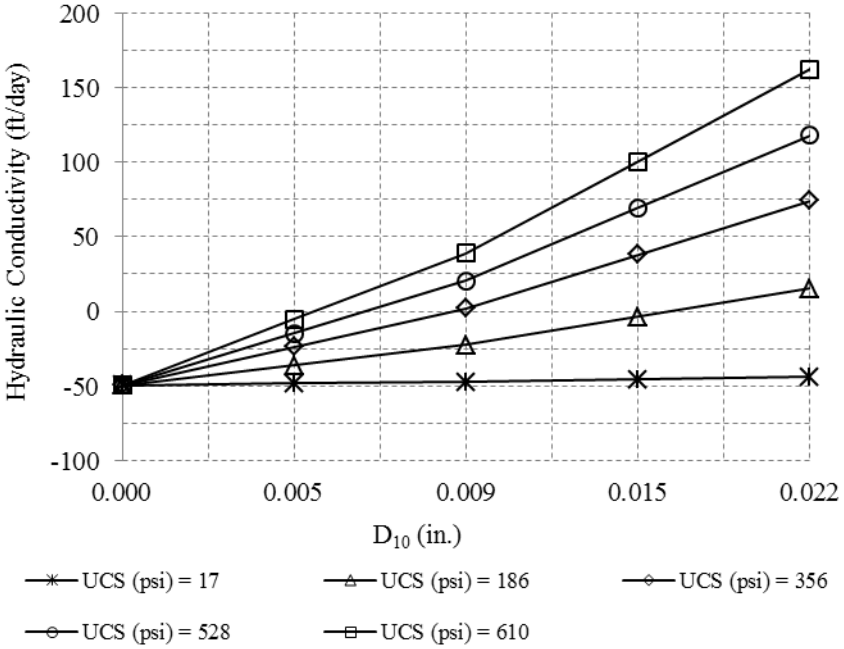

(b)

Figure D-3: Three-way interaction between D_{10}, 7-day UCS, and Unified soil classification for USCS model: (a) GP-GM, (b) GW, (c) ML, (d) SM, and (e) SP.

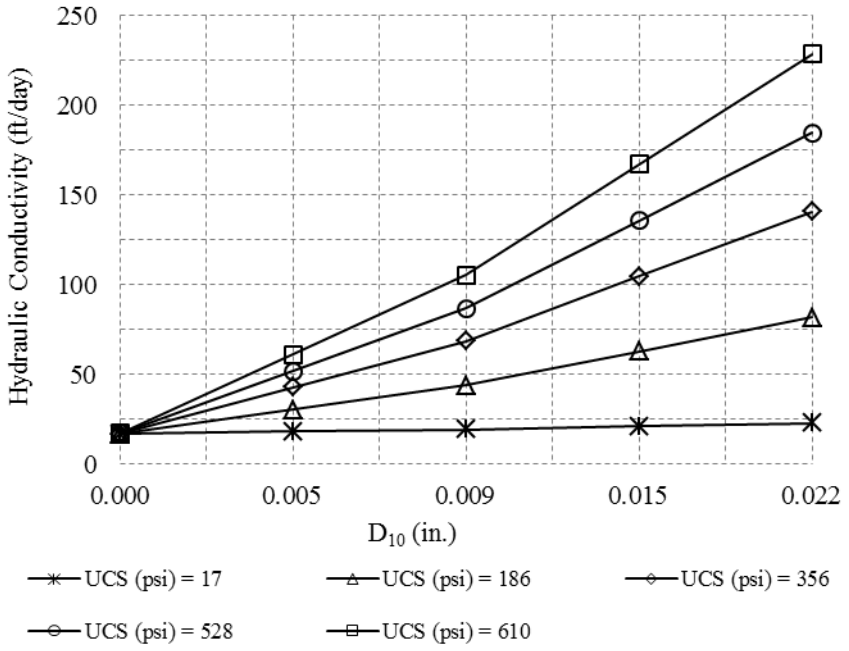

(c)

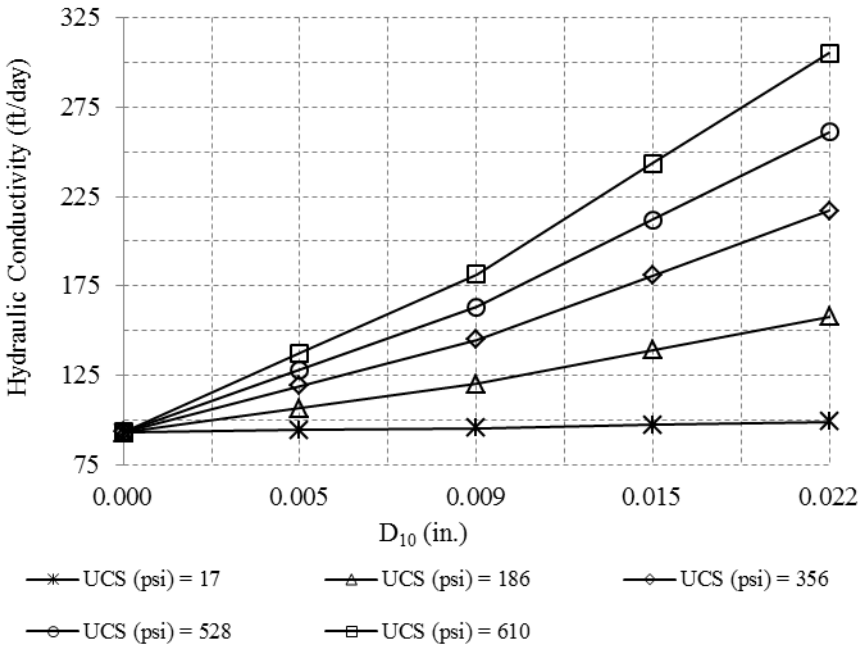

(d)

Figure D-3: (continued.)

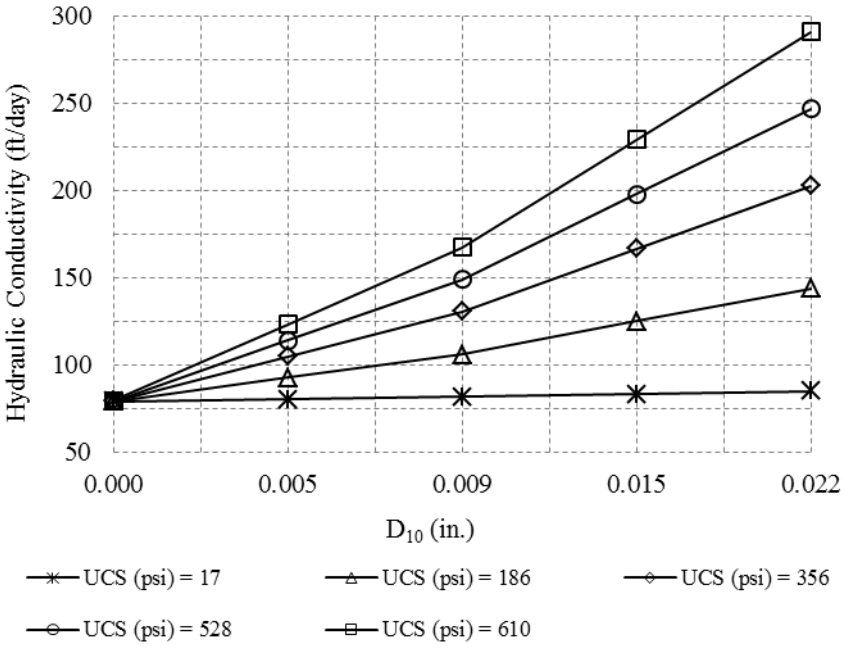

(e)

Figure D-3: (continued.)

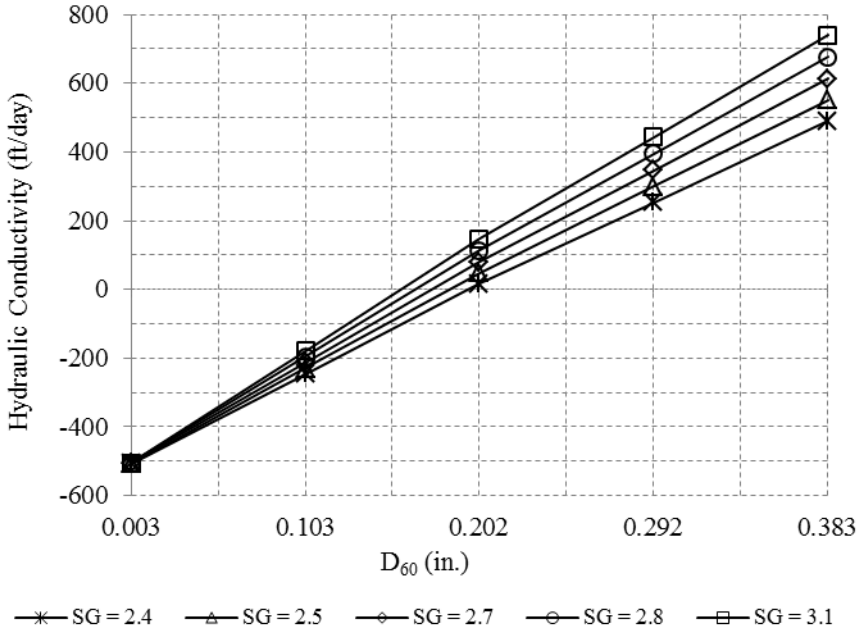

(a)

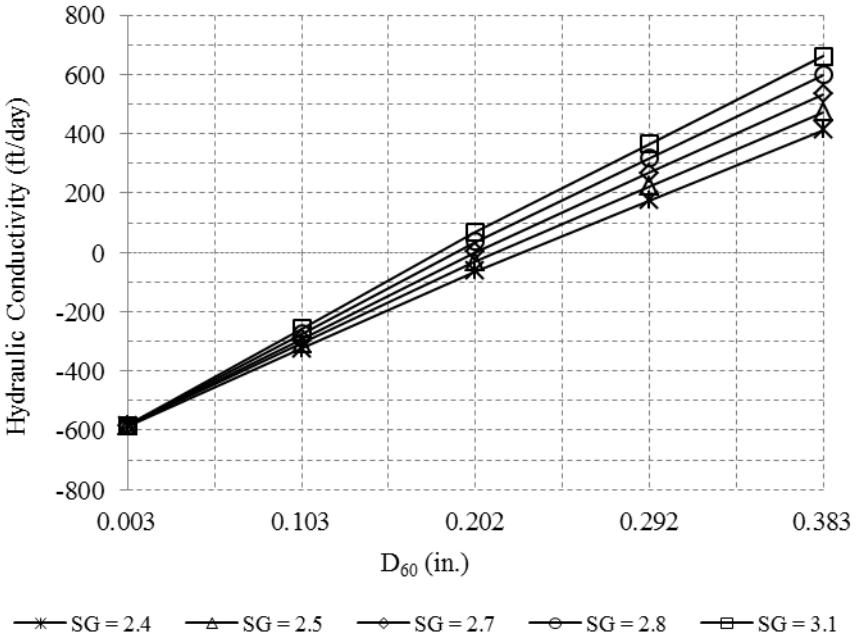

(b)

Figure D-4: Three-way interaction between D_{60}, SG, and Unified soil classification for USCS model: (a) GP-GM, (b) GW, (c) ML, (d) SM, and (e) SP.

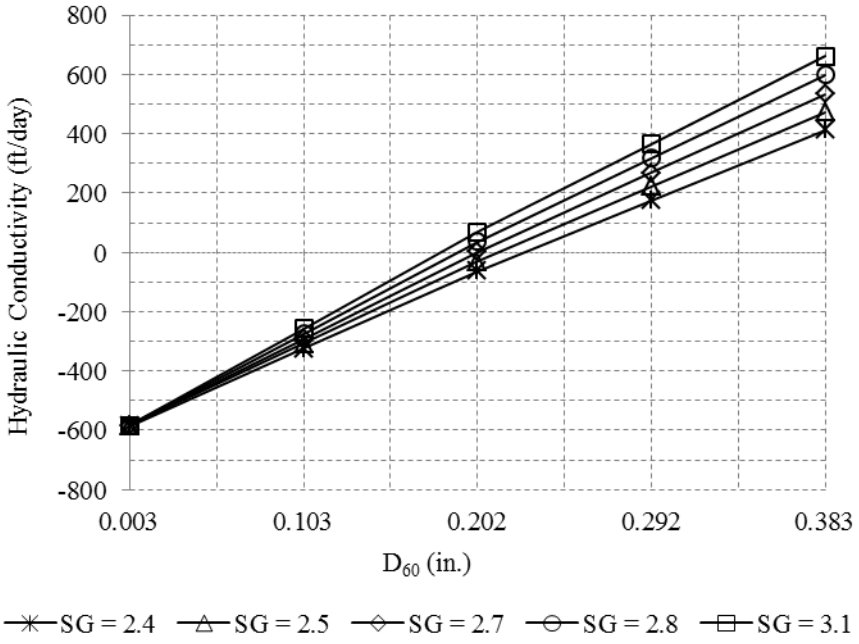

(c)

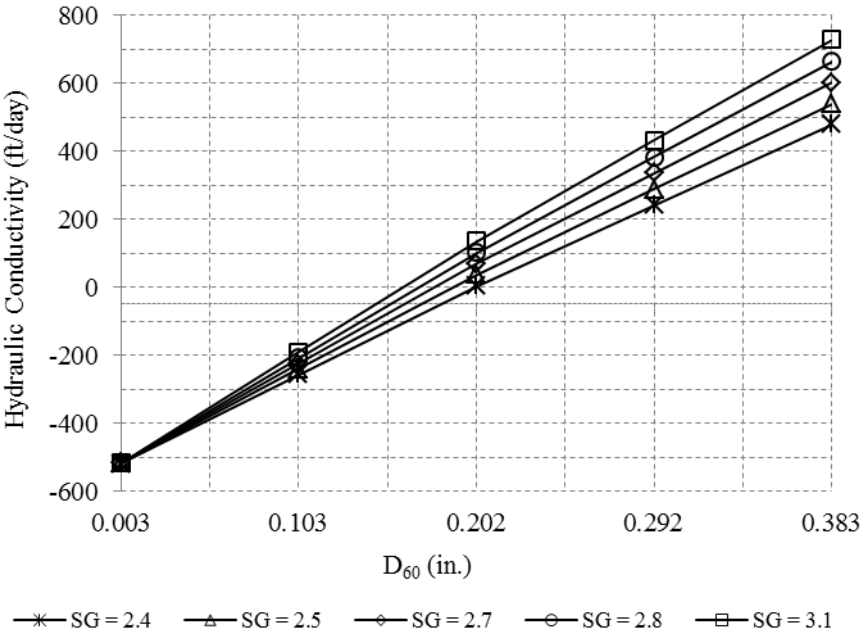

(d)

Figure D-4: (continued.)

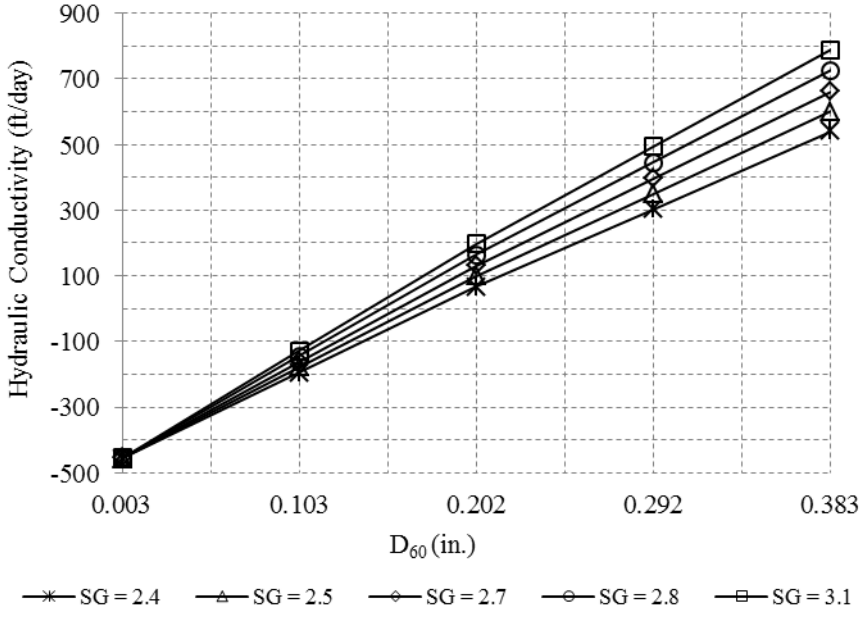

(e)

Figure D-4: (continued.)

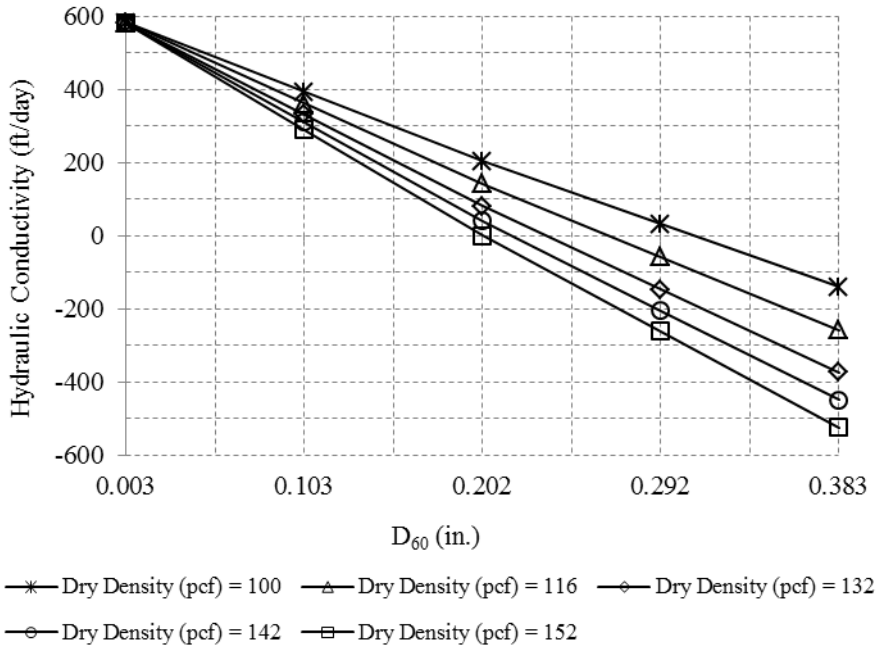

(a)

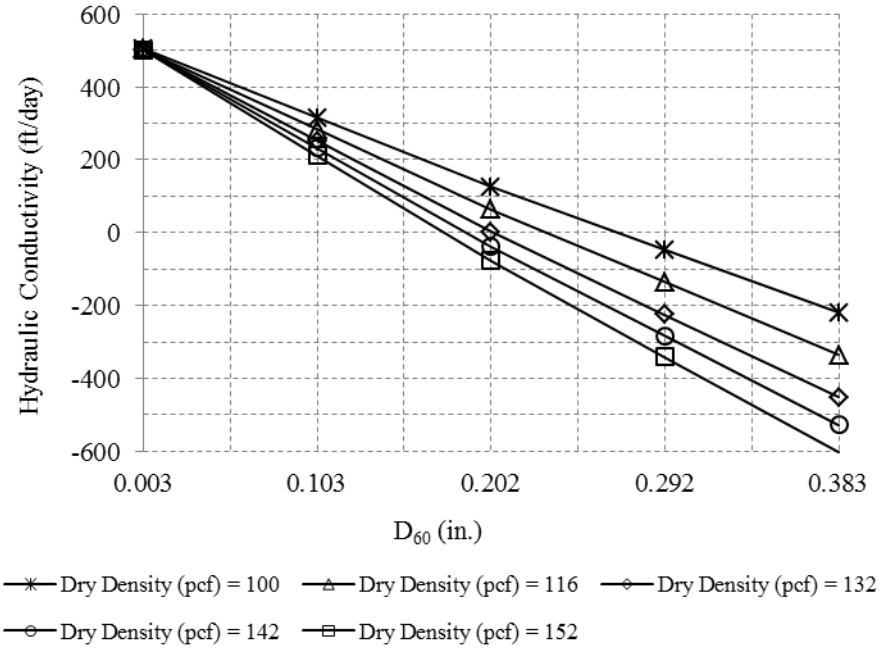

(b)

Figure D-5: Three-way interaction between D_{60}, dry density, and Unified soil classification for USCS model: (a) GP-GM, (b) GW, (c) ML, (d) SM, and (e) SP.

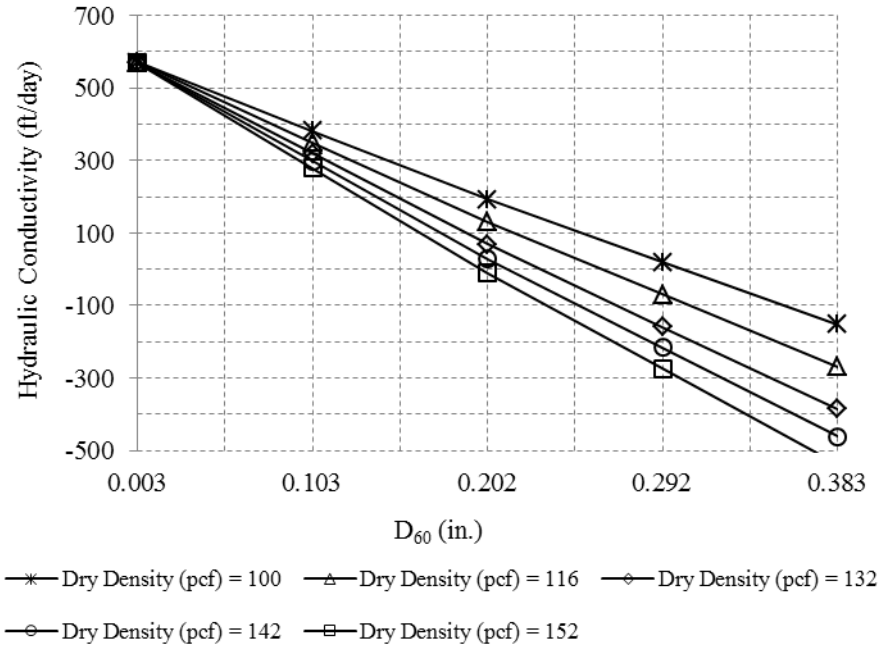

(c)

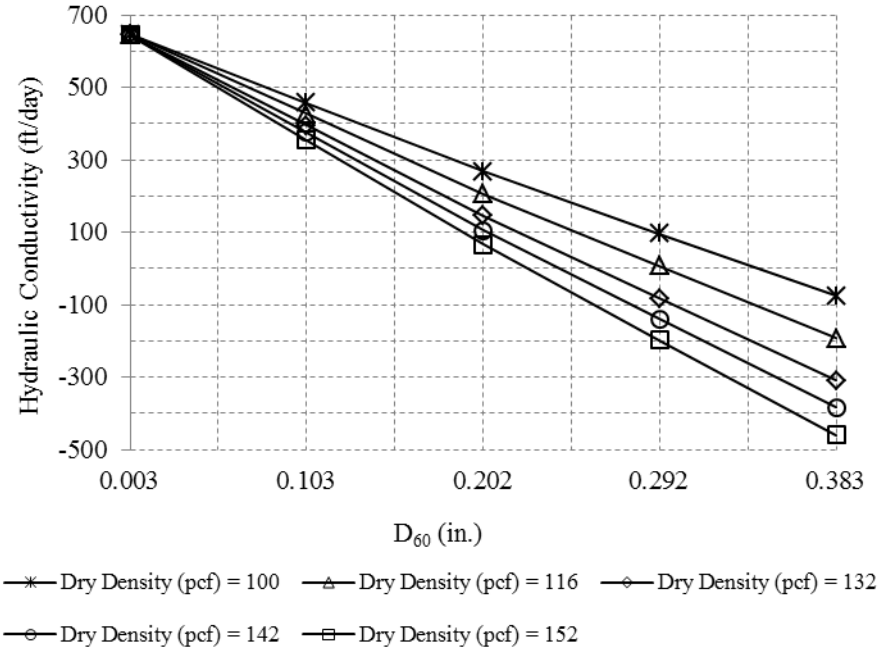

(d)

Figure D-5: (continued.)

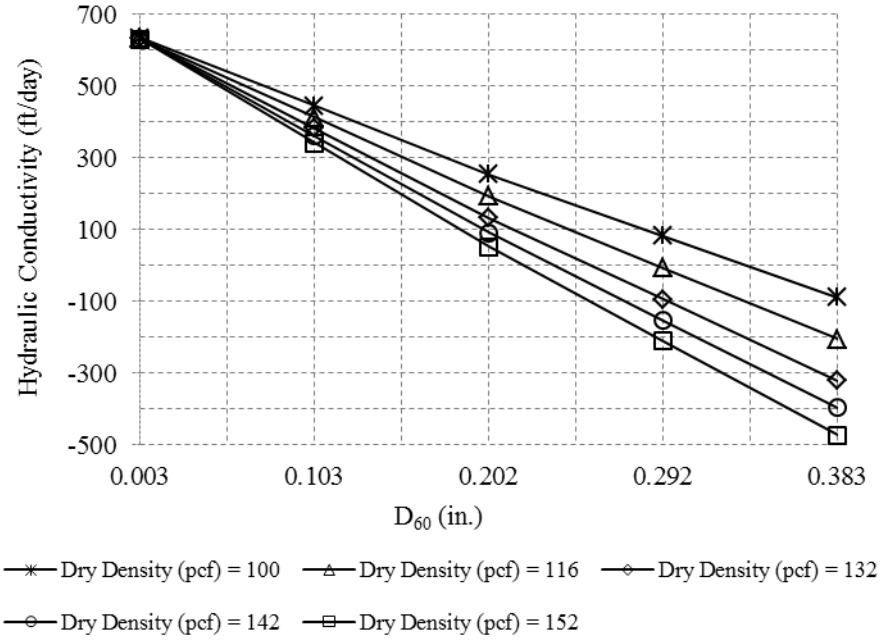

(e)

Figure D-5: (continued.)

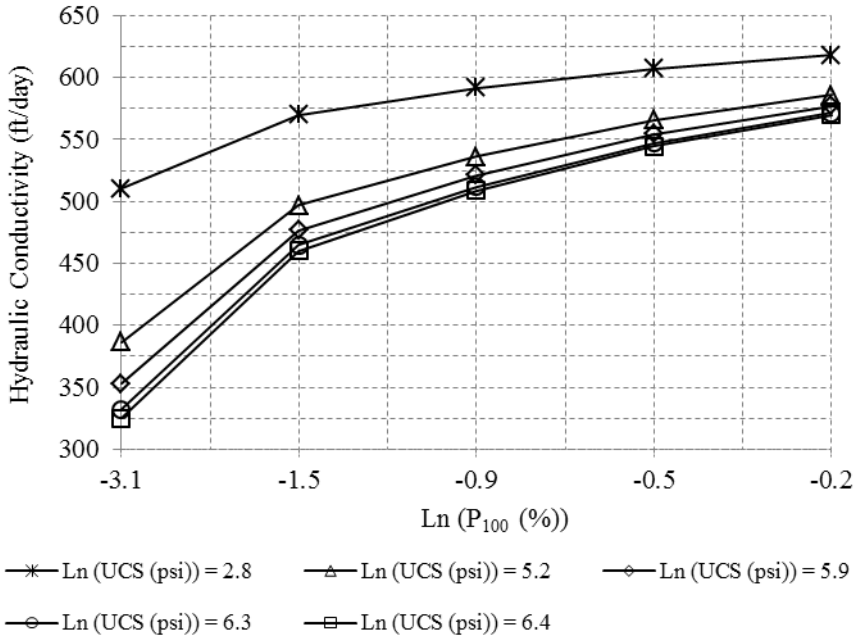

(a)

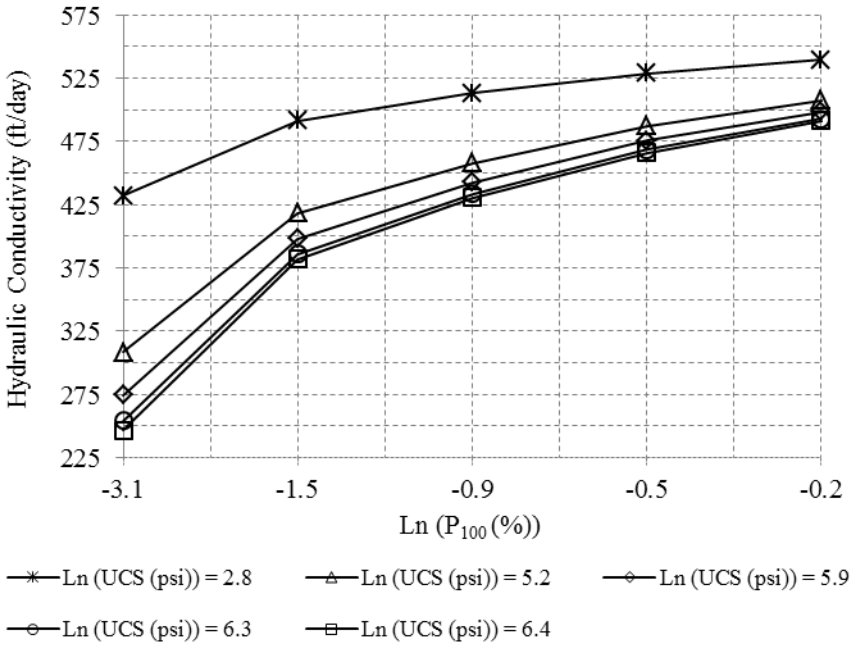

(b)

Figure D-6: Three-way interaction between Ln P_{100}, Ln 7-day UCS, and Unified soil classification for USCS model: (a) GP-GM, (b) GW, (c) ML, (d) SM, and (e) SP.

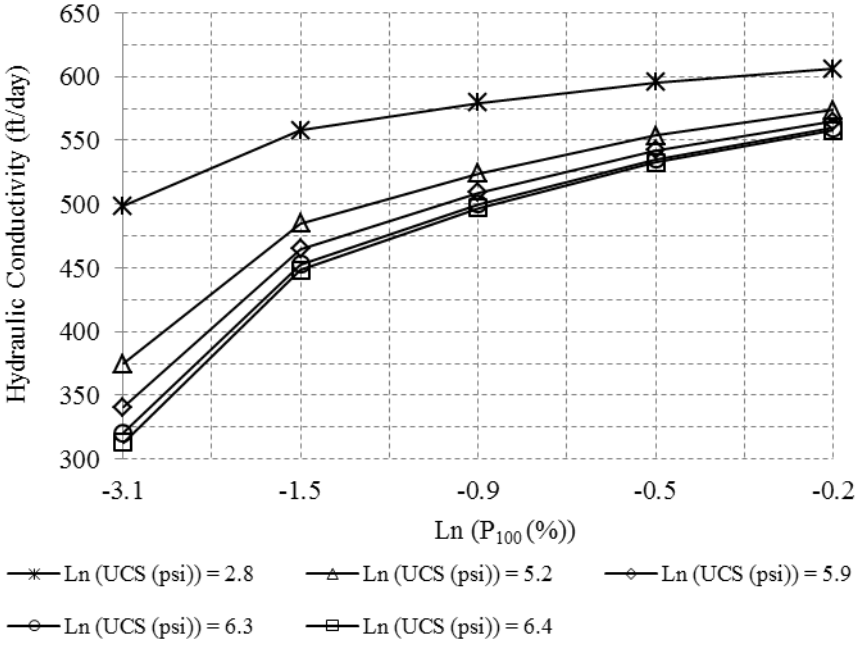

(c)

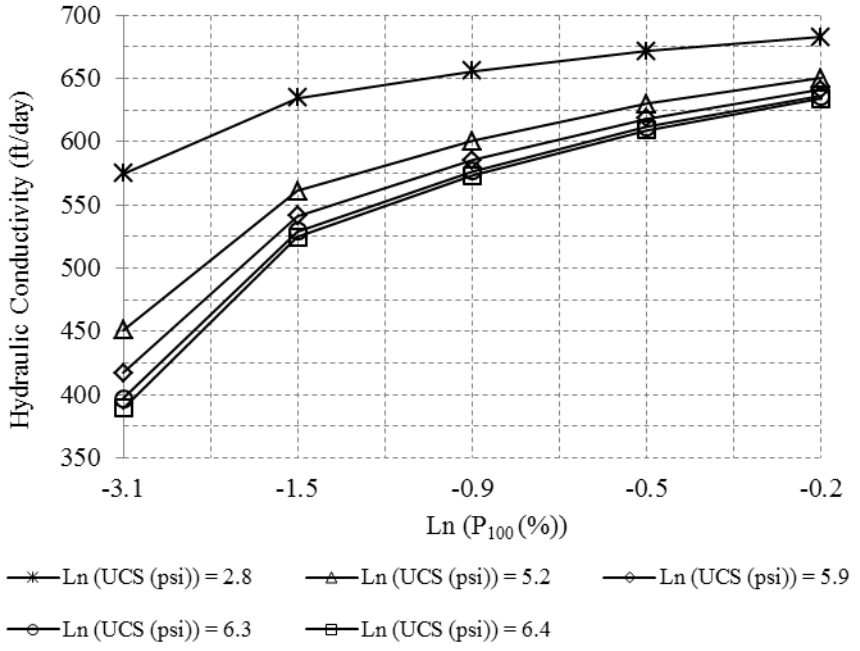

(d)

Figure D-6: (continued.)

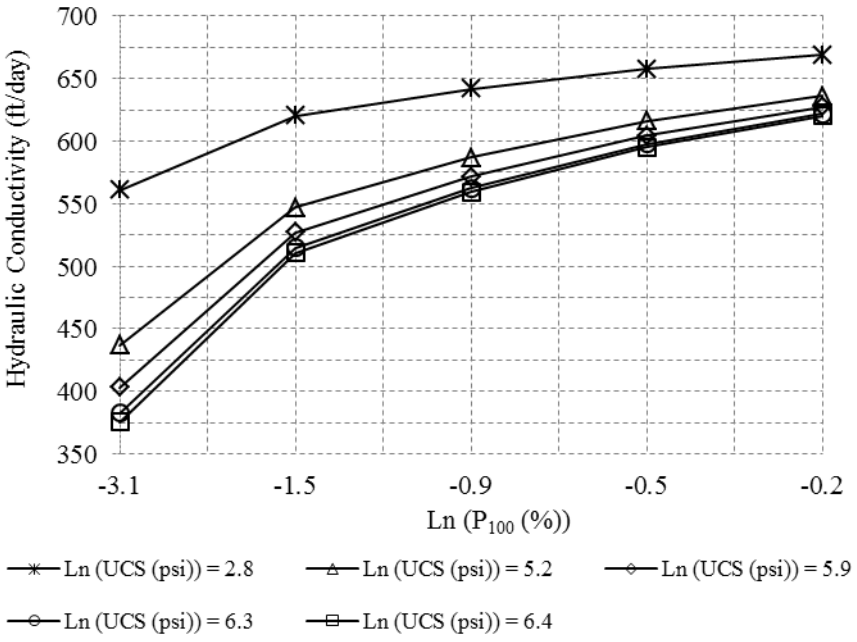

(e)

Figure D-6: (continued.)

APPENDIX E: HYDRAULIC CONDUCTIVITY RESULTS FROM AASHTO-CLASSIFICATION MODEL

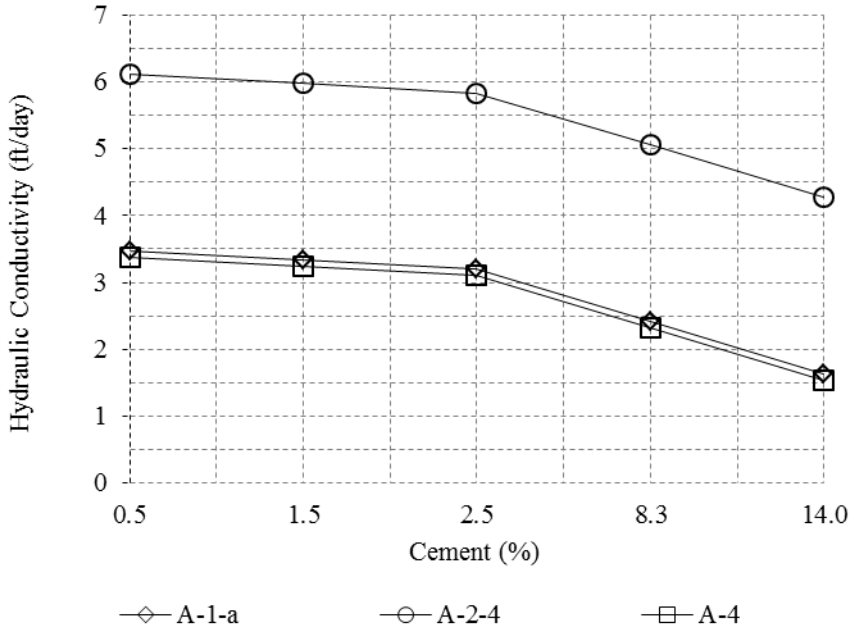

Figure E-1: Two-way interaction between cement content and AASHTO classification for AASHTO-classification model.

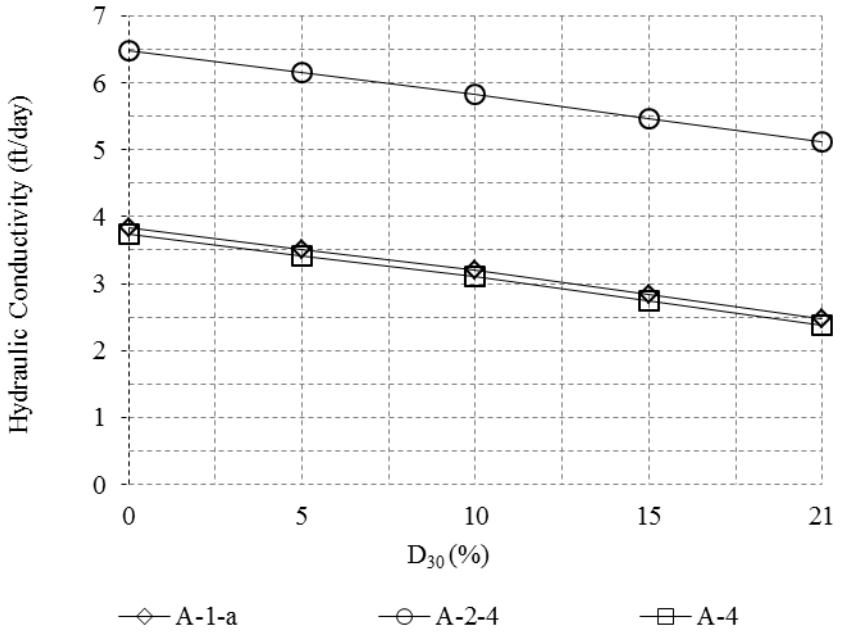

Figure E-2: Two-way interaction between D_{30} and AASHTO classification for AASHTO-classification model.

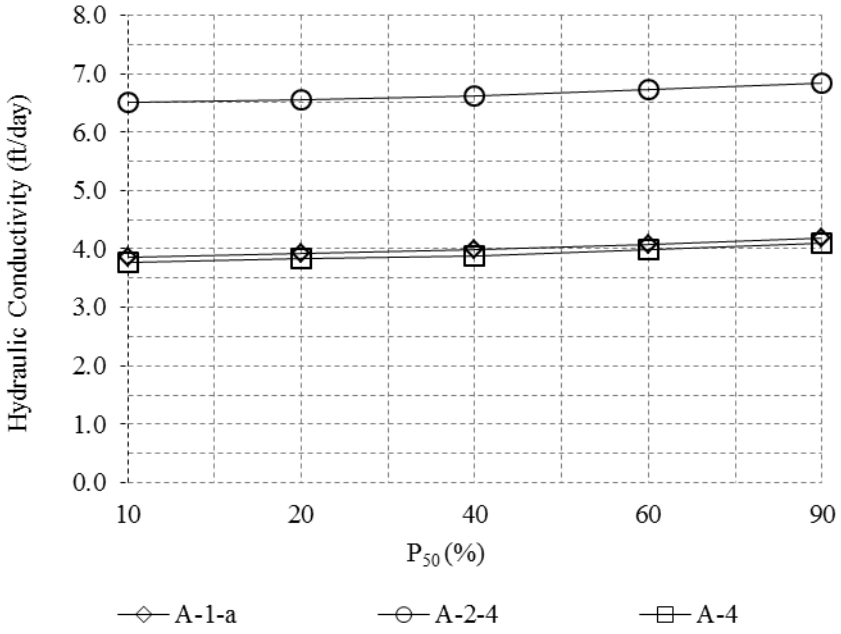

Figure E-53: Two-way interaction between P_{50} and AASHTO classification for AASHTO-classification model.

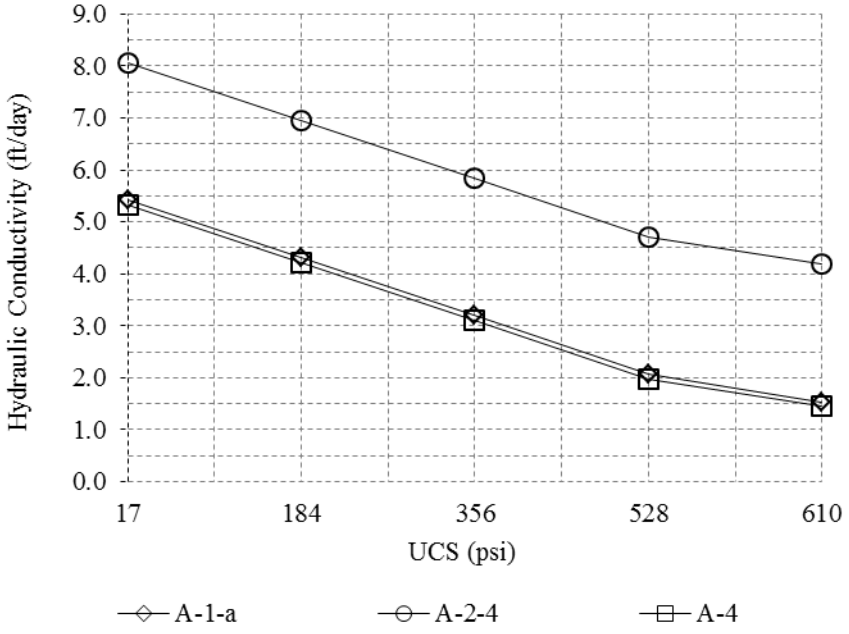

Figure E-4: Two-way interaction between 7-day UCS and AASHTO classification for AASHTO-classification model.

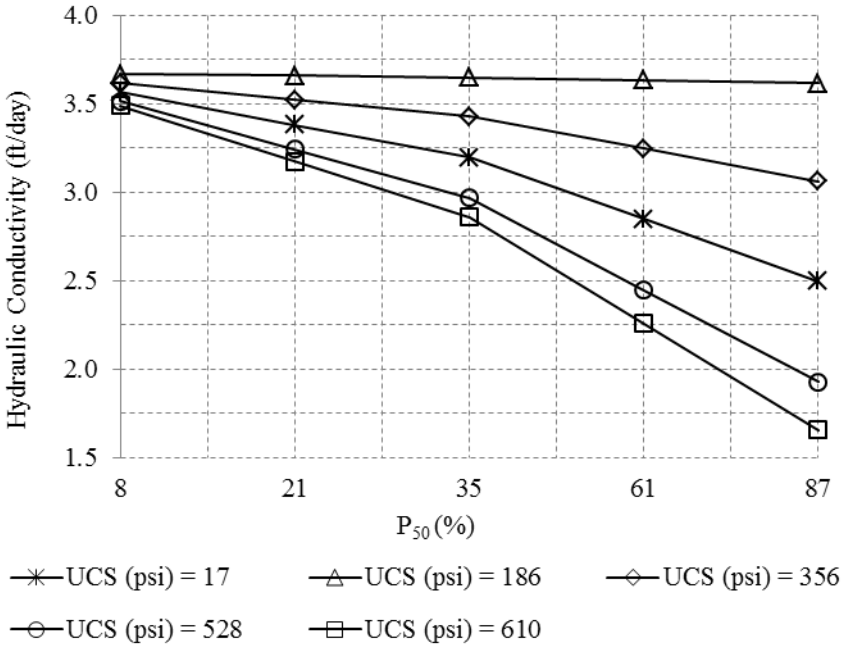

(a)

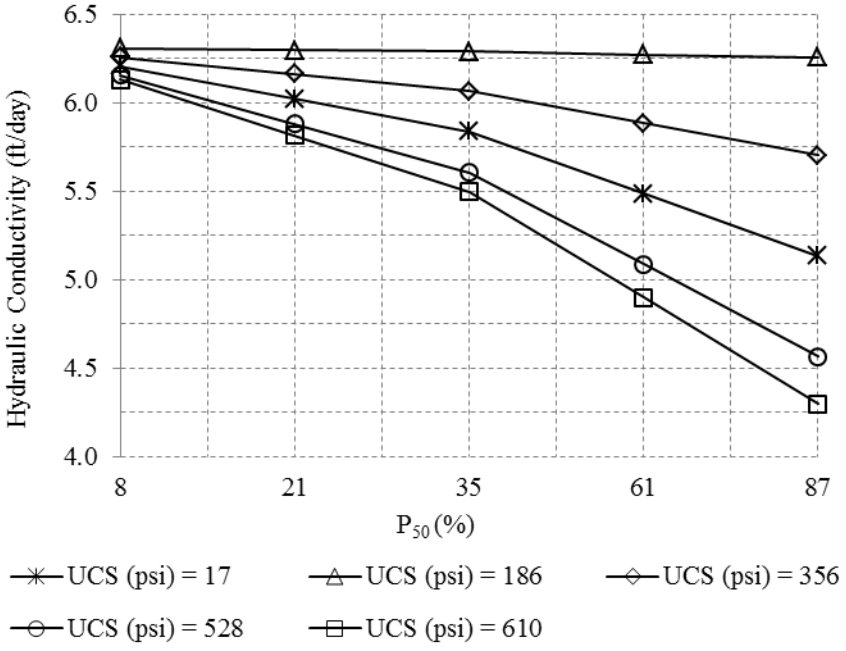

(b)

Figure E-5: Three-way interaction between P_{50}, 7-day UCS, and AASHTO classification for AASHTO-classification model: (a) A-1-a, (b) A-2-4, and (c) A-4.

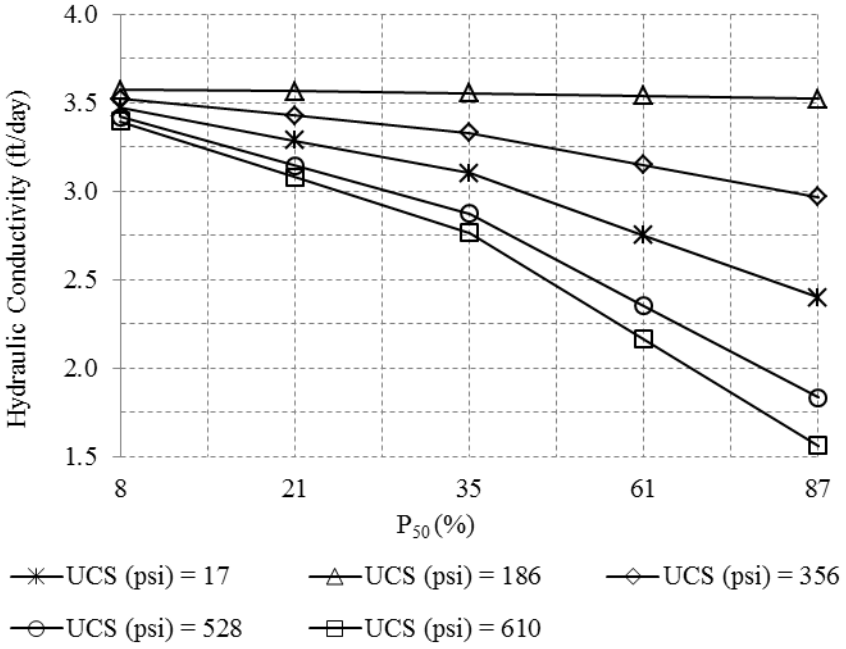

(c)

Figure E-5: (continued.)

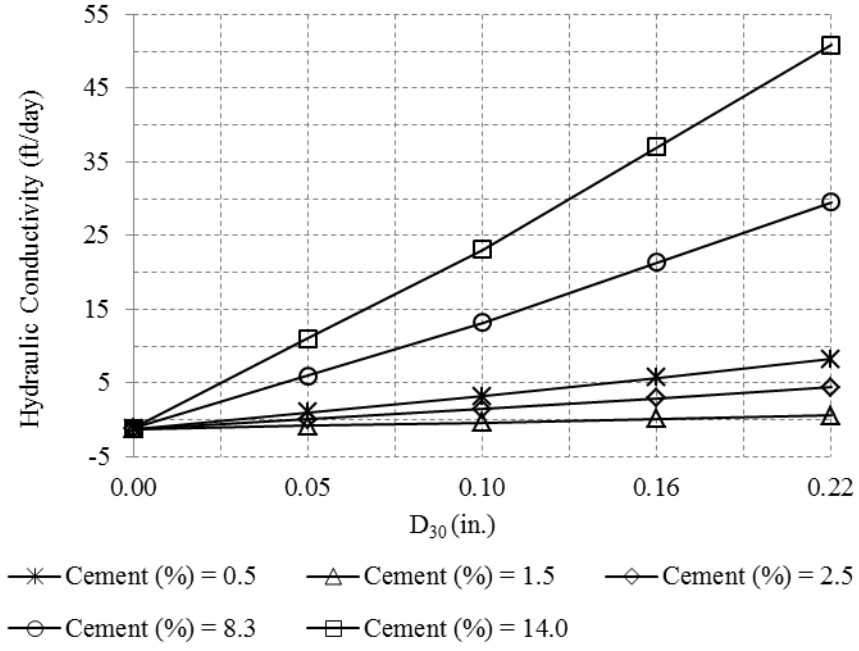

(a)

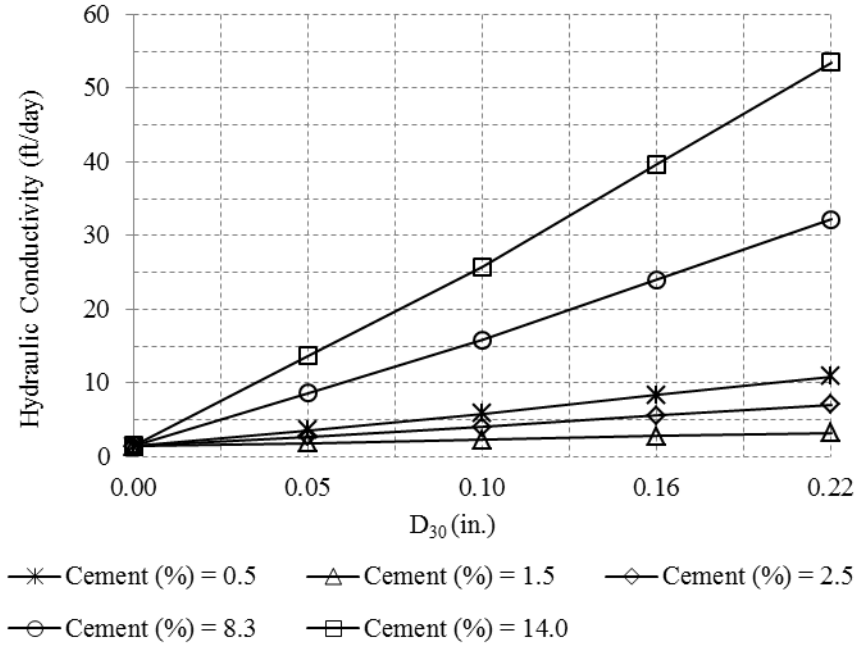

(b)

Figure E-6: Three-way interaction between D_{30}, cement, and AASHTO classification for AASHTO-classification model: (a) A-1-a, (b) A-2-4, and (c) A-4.

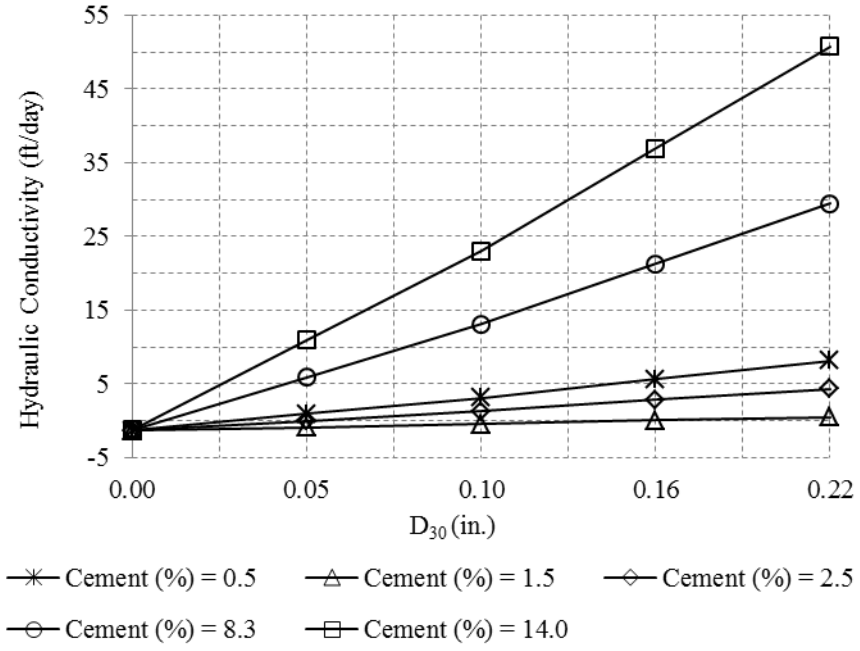

(c)

FIGURE E-6: (continued.)